AD-A119 349 AEROSPACE CORP EL SEGUNDO CA VEHICLE ENGINEERING DIV F/G 12/1
DEVELOPMENT OF AN ANALYTICAL MODEL FOR LARGE SPACE STRUCTURES.(U)
MAR 82 M ASWANI F04701-81-C-0082
UNCLASSIFIED TR-0082(9975)-1 SD-TR-82-59 NL

1 OF 2
AD A
119349

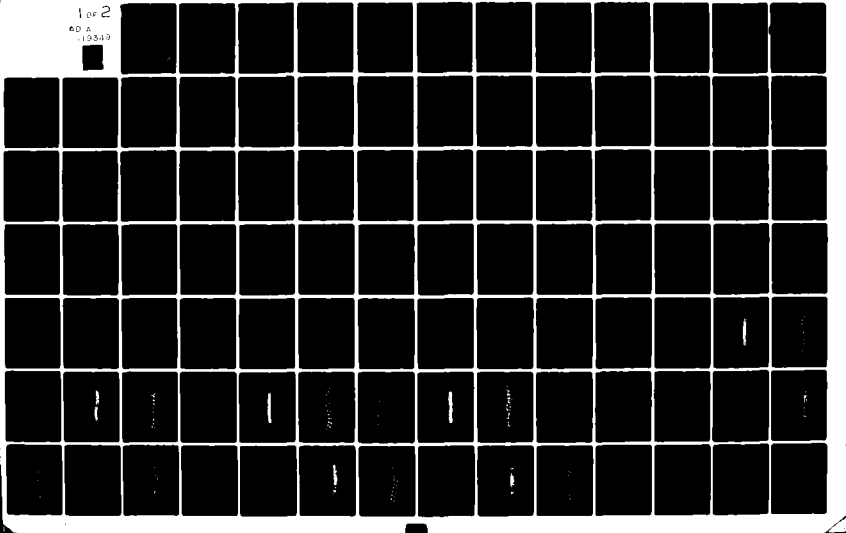

REPORT SD-TR-82-59

(12)

Development of an Analytical Model for Large Space Structures

MOHAN ASWANI
Vehicle Engineering Division
Engineering Group
The Aerospace Corporation
El Segundo, Calif. 90245

15 March 1982

Final Report

October 1980 — September 1981

Prepared for

SPACE DIVISION
AIR FORCE SYSTEMS COMMAND
Los Angeles Air Force Station
P.O. Box 92960, Worldway Postal Center
Los Angeles, Calif. 90009

This final report was submitted by The Aerospace Corporation, El Segundo, CA 90245, under Contract No. F04701-81-C-0082 with the Space Division, Deputy for Technology, P.O. Box 92960, Worldway Postal Center, Los Angeles, CA 90009. It was reviewed and approved for The Aerospace Corporation by H.G. Maier, Principal Director, Vehicle Integrity Subdivision. 2nd Lt Steven G. Hancock, SD/YLXT, was the project officer.

This report has been reviewed by the Public Affairs Office (PAS) and is releasable to the National Technical Information Service (NTIS). At NTIS, it will be available to the general public, including foreign nations.

This technical report has been reviewed and is approved for publication. Publication of this report does not constitute Air Force approval of the report's findings or conclusions. It is published only for the exchange and stimulation of ideas.

Steven G. Hancock

Steven G. Hancock, 2nd Lt, USAF
Project Officer

Jimmie H. Butler

Jimmie H. Butler, Colonel, USAF
Director of Space Systems Technology

FOR THE COMMANDER

Norman W. Lee, Jr

Norman W. Lee, Jr, Colonel, USAF
Deputy for Technology

UNCLASSIFIED

SECURITY CLASSIFICATION OF THIS PAGE (When Data Entered)

REPORT DOCUMENTATION PAGE	READ INSTRUCTIONS BEFORE COMPLETING FORM
1. REPORT NUMBER: SD-TR-82-59	2. GOVT ACCESSION NO.: AD A119347
	3. RECIPIENT'S CATALOG NUMBER:
4. TITLE (and Subtitle): DEVELOPMENT OF AN ANALYTICAL MODEL FOR LARGE SPACE STRUCTURES	5. TYPE OF REPORT & PERIOD COVERED: Final Report October 1980-September 1981
	6. PERFORMING ORG. REPORT NUMBER: TR-0082(9975)-1
7. AUTHOR(s): Mohan Aswani	8. CONTRACT OR GRANT NUMBER(s): F04701-81-C-0082
9. PERFORMING ORGANIZATION NAME AND ADDRESS: The Aerospace Corporation, El Segundo, CA 90245	10. PROGRAM ELEMENT, PROJECT, TASK AREA & WORK UNIT NUMBERS:
11. CONTROLLING OFFICE NAME AND ADDRESS:	12. REPORT DATE: 15 March 1982
	13. NUMBER OF PAGES: 93
14. MONITORING AGENCY NAME & ADDRESS (if different from Controlling Office): Space Division, Air Force Systems Command, Los Angeles Air Force Station, P.O. Box 92960 Worldway Postal Center, Los Angeles, CA 90009	15. SECURITY CLASS. (of this report): Unclassified
	15a. DECLASSIFICATION DOWNGRADING SCHEDULE:

16. DISTRIBUTION STATEMENT (of this Report)

Approved for public release; distribution unlimited.

17. DISTRIBUTION STATEMENT (of the abstract entered in Block 20, if different from Report)

18. SUPPLEMENTARY NOTES

19. KEY WORDS (Continue on reverse side if necessary and identify by block number)

Large Space Structures	Mode Shapes	Rotary Inertia
Equivalent Continuum Model	Constitutive Equations	Tetrahedral Truss
Free Vibration	Plate Theory	Equivalent Stiffness
Natural Frequency	Transverse Shear	Finite Element Model

20. ABSTRACT (Continue on reverse side if necessary and identify by block number)

A methodology is presented for modeling large truss-type structures based on the concept of equivalent continuum. The equivalent effective elastic and dynamic properties of the continuum model in terms of the material and geometric properties of the truss are derived in a simple and straightforward manner. The accuracy of the model is demonstrated in a free vibration problem, when the results are compared to those obtained from the conventional finite

DD FORM 1473 (FACSIMILE)

UNCLASSIFIED

SECURITY CLASSIFICATION OF THIS PAGE (When Data Entered)

19 KEY WORDS (Continued)

20 ABSTRACT (Continued)

element method. Both simply supported and free-free boundary conditions are considered. In addition, the assumptions made in obtaining the continuum solution are discussed. Numerical results clearly indicate the potential of this approach for modeling large repetitive truss-type structures.

PREFACE

The author wishes to express his appreciation to Mr. N. N. Au, Director of the Structures Department, for not only the initiation of this study, but also for the valuable suggestions and the direction in carrying out this investigation. The helpful comments and encouragement provided by Dr. S. R. Lin, Manager of the Thermostructural Analysis Section, are gratefully acknowledged. Appreciation is also extended to Dr. R. N. Coppolino and Mr. Werner Herbig for reviewing this report.

The computer programming help of Mr. R. Crespo, secretarial assistance of Ms. Nancy Del Regno, Word Processing Services of Mrs. Stephanie Johnson and Ms. Mary Gainey, and the art work of Ms. Mary Jane McNeil are sincerely appreciated.

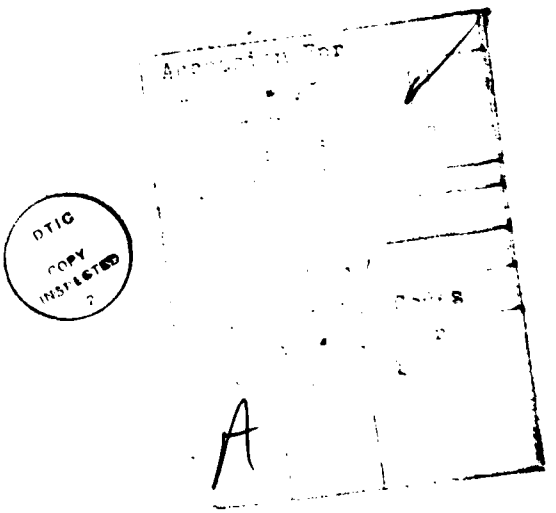

CONTENTS

FIGURES

FIGURES (Continued)

FIGURES (Concluded)

TABLES

I. INTRODUCTION

Large space structures have been identified as having a number of potential applications for national security and future energy needs. Typical applications include solar power station, large space mirror, large space antenna, space-based radar, and multipurpose large space platform. Various missions which require large lightweight structures and the major design requirements of such structures have been summarized by NASA in Refs. 1 and 2. Although prioritized specific missions are yet to be defined, several novel and innovative design concepts have been suggested for future applications (Refs. 3 through 14). These generic conceptual ideas provide valuable information regarding the technology needed for developing structurally efficient low cost systems. The size, design environment, manufacturing methods, and other characteristics associated with large space structures dictate that the first time such a structural system assumes its operational configuration, it will occur in orbit, thus creating unique design and testing problems. Furthermore, the cost involved in deploying such structural assemblies to their full capacity requires a high level of confidence in analytical methods and modeling

---

[1]"Outlook for Space," NASA Task Group, NASA SP-386, January 1976.

[2]Hedgepeth, John M., "Survey of Future Requirements for Large Space Structures," NASA CR-2621, 1975.

[3]Woods, A. A., Jr., "Offset Wrap Rib Concept and Development (LMSC)," Large Space Systems Technology, NASA Conference Publication 2118, 1979.

[4]Archer, J. S., "Advanced Sunflower Antenna Concept Development (TRW)," Large Space Systems Technology, NASA Conference Publication 2118, 1979.

[5]Montgomery, D.C. and L.D. Skides, "Development of Maypole (Hoop/Column) Deployable Reflector Concept for Large Space Systems Applications (Harris Corp.)," Large Space Systems Technology, NASA Conference Publication 2118, 1979.

[6]"Modular Reflector Concepts Study (GDC)," Large Space Systems Technology, NASA Conference Publication 2118, 1979.

techniques for predicting their structural responses to the natural and induced environments. Although significant emphasis has been placed on developing design concepts, construction methodology, and deployment techniques for large space structures, extremely limited efforts have been devoted to developing efficient analytical methods for structural modeling. As currently envisioned, a strong candidate for a large low-mass and high-stiffness structure is an open truss configuration. The design, analysis, and testing of such a structure, with a large number of structural elements, present several challenging problems. Some such problems are to develop capabilities for conveniently assessing preliminary designs, efficiently carrying out tradeoff studies, confidently predicting structural responses, suitably designing ground test methodology, and judiciously recommending space verification test programs.

---

[7]"DOD/STS On-Orbit Assembly Concept Design Study (GDC)," SAMSO-TR-78-128, 1978.

[8]"DOD/STS On-Orbit Assembly Concept Design Study (MMC)," Martin Marietta Corporation, Report MCR-78-113, 1978.

[9]Agan, W. E., "Erectable/Deployable Concepts for Large Space System Technology (Vought Corp.)," Large Space System Technology, NASA Conference Publication 2118, 1979.

[10]Britton, W. R. and J. D. Johnston, "Space Spider - A Concept for Fabrication of Large Space Structures," AIAA Conference on Large Space Platforms: Future Needs and Capabilities, September 1978.

[11]Stokes, J. W. and E. C. Pruett, "Structural Assembly in Space," Large Space Systems Technology, NASA Conference Publication 2118, 1979.

[12]Nein, M. E. and F. C. Runge, "Science and Applications Space Platforms," AIAA 81-0458, AIAA Second Conference on Large Space Platforms, February 1981.

[13]Johnson, R. R., H. Cohan, and G. G. Jacquemin, "A Concept for High Speed Assembly for Erectable Space Platforms," AIAA 81-0446, AIAA Second Conference on Large Space Platforms, February 1981.

[14]Stoll, H. W., Systematic Design of Deployable Structures," AIAA 81-0444, AIAA Second Conference on Large Space Platforms, February 1981.

Essentially three methods are available for analyzing truss-type structures: a direct approach, a discrete field approach, and a continuum approach. In the direct approach, a structure is analyzed as a system of discrete elements, and the usual techniques for solving structural framework problems are applied. The method has obvious limitations in that for a large structure it involves the solution of a very large system of equations, which is both time-consuming and expensive. The discrete field approach takes advantage of the regularity of the structure. It is an extension of the classical method used for continuum problems in which equilibrium and compatibility equations at each node (or joint) of the structural frame are formulated first and then the resulting governing equations for the total system are solved using finite differences and differential calculus.

The state of the art of the discrete field method is summarized in Ref. 15, whereas some example problems illustrating this approach are given in Refs. 16 through 18. Although the discrete field method is useful for moderate-sized problems with simple geometry, it becomes increasingly complex when applied to large intricate configurations.

---

[15]Dean, D. L. and R. R. Avent, "State-of-the-Art of Discrete Field Analysis of Space Structures," Proceedings of Second International Conference on Space Structures. Edited by W. J. Supple, University of Surrey, Guildford, England, September 1975.

[16]Renton, J. D., "The Related Behavior of Plane Grids, Space Grids, and Plates," Space Structures, Blackwell, Oxford, England, 1967.

[17]Renton, J. D, "General Properties of Space Grids," International Journal of Mechanical Sciences, Vol. 12, 1970.

[18]Dean, D. L. and C. P. Ugarte, "Field Solutions for Two-Dimensional Framework," International Journal of Mechanical Sciences, Vol. 10, 1968.

The third approach is a technique to replace discrete structural frameworks with equivalent continuum models (Refs. 19 through 25). It involves the determination of equivalent elastic and dynamic properties of the truss structure. The response of a given structure is then predicted by solving the continuum model under similar loading and boundary conditions. The continuum problem can, in general, be simplified by making certain logical kinematic assumptions. For example, a large platform-type truss could be modeled as an equivalent continuum plate, whereas a long truss boom could be represented by an equivalent continuum beam. This approach, when applied to large space structures, has great versatility in efficiently determining the overall response of the structure to the induced loading as well as in carrying out the design feasibility and tradeoff studies. Although much work has yet to be done toward accomplishing "perfection," the present study represents a step forward in the state of the art of developing modeling methodology for large truss-type structures based on the equivalent continuum approach.

---

[19]Mikulas, M. M., Jr., H. G. Bush, and M. F. Card, "Structural Stiffness Strength and Dynamic Characteristics of Large Tetrahedral Space Truss Structures," NASA TMX74001, 1977.

[20]Bush, H. G., M. M. Mikulas, Jr., and W. L. Heard, "Some Design Considerations for Large Space Structures," Proceedings of the AIAA/ASME 18th Structures, Structural Dynamics, and Materials Conference, Vol. A, 1977.

[21]Renton, J. D., "On the Gridwork Analogy for Plates," Journal of Mechanics, Physics, and Solids, Vol. 13, 1965.

[22]Flower, W. R., and L. C. Schmidt, "Analysis of Space Truss as Equivalent Plate," Journal of the Structural Division, Vol. 97, ASCE, 1971.

[23]Heki, K., "On the Effective Rigidities of Lattice Plates," Recent Researches of Structural Mechanics, Tokyo, 1968.

[24]Sun, C. T., and T. Y. Yang, "A Continuum Approach Toward Dynamics of Gridworks," Journal of Applied Mechanics, Vol. 91, ASME, 1965.

[25]Nayfeh, A. H. and M. S. Hefzy, "Continuum Modeling of Three-Dimensional Truss-Like Space Structures," AIAA Journal, Vol. 16, No. 8, 1979.

The procedure for deriving the effective elastic and dynamic properties of an equivalent continuum model is given in Section II, while the analytical solution of the equivalent continuum model is discussed in Section III. An example problem for verifying accuracy of the model is illustrated in Section IV followed by the conclusions of this study.

II. EQUIVALENT CONTINUUM MODEL

A. DETERMINATION OF EQUIVALENT EFFECTIVE PROPERTIES

The procedure for determining the effective properties of an equivalent continuum model, similar to that of Nayfeh and Hefzy (Ref. 26), was independently derived. The approach is straightforward. For a given truss structure, all sets of parallel members are identified. The direction cosines for each set of parallel members are determined with respect to the global reference coordinate system. Unidirectional stiffness properties of each set are derived next by "smearing" the stiffness of individual members in the set over the effective area. Finally, through orthogonal transformations, contributions of each set to the effective continuum properties are derived.

For a linear elastic body, the stress-strain relations are given by

$$\sigma_{ij} = C_{ijk\ell}\,\epsilon_{k\ell} \qquad i,j,k,\ell = 1,2,3 \tag{1}$$

where σ_{ij} and $\epsilon_{k\ell}$ are the components of stress and strain tensor, respectively, and $C_{ijk\ell}$ are the elastic constants. Equation (1), in matrix form, is written as

$$\begin{Bmatrix} \sigma_{11} \\ \sigma_{22} \\ \sigma_{33} \\ \sigma_{23} \\ \sigma_{31} \\ \sigma_{12} \end{Bmatrix} = \begin{bmatrix} C_{1111} & C_{1122} & C_{1133} & C_{1123} & C_{1131} & C_{1112} \\ C_{2211} & C_{2222} & C_{2233} & C_{2223} & C_{2231} & C_{2212} \\ C_{3311} & C_{3322} & C_{3333} & C_{3323} & C_{3331} & C_{3312} \\ C_{2311} & C_{2322} & C_{2333} & C_{2323} & C_{2331} & C_{2312} \\ C_{3111} & C_{3122} & C_{3133} & C_{3123} & C_{3131} & C_{3112} \\ C_{1211} & C_{1222} & C_{1233} & C_{1223} & C_{1212} & C_{1212} \end{bmatrix} \begin{Bmatrix} \epsilon_{11} \\ \epsilon_{22} \\ \epsilon_{33} \\ \epsilon_{23} \\ \epsilon_{31} \\ \epsilon_{12} \end{Bmatrix} \tag{2}$$

---

[26] Nayfeh, A. H., and M. S. Hefzy, "Continuum Modeling of the Mechanical and Thermal Behavior of Discrete Large Structures," AIAA 80-0679, AIAA/ASME/ASCE/AHS 21st Structures, Structural Dynamics, Materials Conference, May 12-14, 1980.

An expression for determining $C_{ijk\ell}$ for an equivalent continuum in terms of the geometric and material properties of the original structure shall now be derived. If $(\beta_{ij})_m$ are the direction cosines of the m^{th} parallel member set and $(C'_{pqrs})_m$ are the smeared stiffness properties of that set, the global contributions $(C_{ijk\ell})_m$ of this set to the effective equivalent continuum properties are given by

$$(C_{ijk\ell})_m = (\beta_{ip}\,\beta_{jq}\,\beta_{kr}\,\beta_{\ell s})_m (C'_{pqrs})_m \tag{3}$$

where

$$(\beta_{ij})_m = \left(\frac{\partial x'_i}{\partial x_j}\right)_m \tag{4}$$

or alternatively

$$(\beta_{ij})_m = [\cos(x'_i\ ,\ x_j)]_m \tag{5}$$

where x_j and x'_i are the global and local coordinates, respectively.

Equation (3) can be further simplified. Because, in truss structures, the members have only one unidirectional elastic property C'_{1111} (the modulus of elasticity along the principal direction of the truss member) Eq. (3) can be rewritten as

$$(C_{ijk\ell})_m = (\beta_{i1}\,\beta_{j1}\,\beta_{k1}\,\beta_{\ell 1})_m (C'_{1111})_m \tag{6}$$

B. DETERMINATION OF $(C'_{1111})_m$

The effective unidirectional elastic property of a set of parallel rods, Fig. 1, spaced a_m apart is given by

$$(C'_{1111})_m = \frac{E_m A_m}{a_m h} \tag{7}$$

and the effective mass density is given by

$$\rho'_m = \frac{\rho_m A_m}{a_m h} \tag{8}$$

where A_m is the cross-sectional area, E_m is the modulus of elasticity, and ρ_m is the mass density of the members of the m^{th} parallel member set. The linear dimension h is a reference measurement introduced for the purpose of obtaining area average.

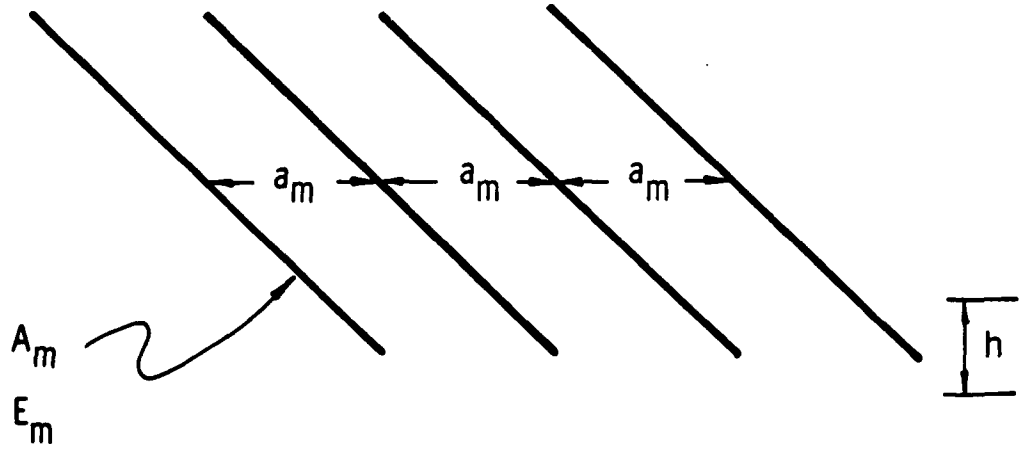

Fig. 1. A Set of Parallel Rods

The equivalent continuum elastic properties C_{ijkl} are now obtained by summing the contributions of all n parallel member sets

$$C_{ijkl} = \sum_{m=1}^{n} (C_{ijkl})_m \tag{9}$$

and the effective mass density is

$$\rho_0 = \sum_{m=1}^{n} \rho'_m \tag{10}$$

C. APPLICATIONS

1. Two-Dimensional Framework

The procedure for obtaining equivalent continuum properties is illustrated through example problems. A two-dimensional framework is shown in Fig. 2. One can easily identify four sets of parallel members. The direction cosines for these four sets, with respect to x_1, x_2 axes, are

$$\begin{aligned}
(\beta_{11})_1 &= 1 & (\beta_{11})_3 &= 1/\sqrt{2} \\
(\beta_{12})_1 &= 0 & (\beta_{12})_3 &= 1/\sqrt{2} \\
(\beta_{11})_2 &= 0 & (\beta_{11})_4 &= 1/\sqrt{2} \\
(\beta_{12})_2 &= 1 & (\beta_{12})_4 &= -1/\sqrt{2}
\end{aligned} \tag{11}$$

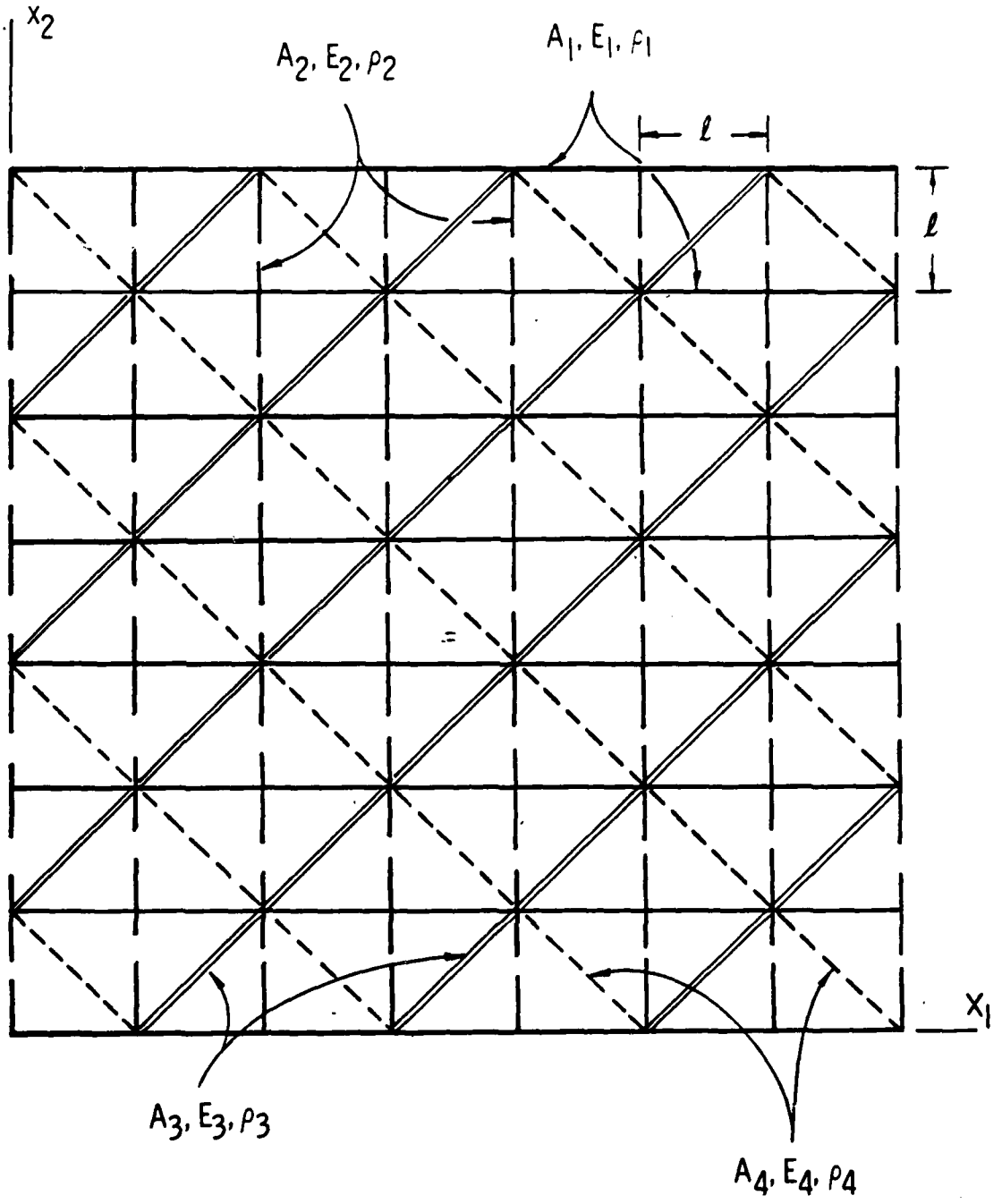

Fig. 2. Two-Dimensional Framework
(0°, 90°, ±45° Arrangement)

If A_m, E_m, and ρ_m (m = 1 through 4) are the cross-sectional area, modulus of elasticity, and mass density, respectively, of the members in these four sets, the effective mass and elastic properties of each set are

$$\rho'_1 = \frac{\rho_1 A_1}{\ell h} \qquad (C'_{1111})_1 = \frac{E_1 A_1}{\ell h}$$

$$\rho'_2 = \frac{\rho_2 A_2}{\ell h} \qquad (C'_{1111})_2 = \frac{E_2 A_2}{\ell h}$$

$$\rho'_3 = \frac{\sqrt{2}}{2} \frac{\rho_3 A_3}{\ell h} \qquad (C'_{1111})_3 = \frac{\sqrt{2}}{2} \frac{E_3 A_3}{\ell h}$$

$$\rho'_4 = \frac{\sqrt{2}}{2} \frac{\rho_4 A_4}{\ell h} \qquad (C'_{1111})_4 = \frac{\sqrt{2}}{2} \frac{E_4 A_4}{\ell h} \tag{12}$$

and all other $(C'_{ijk\ell})_m$ vanish.

From Eqs. (6) and (11)

$$(C_{1111})_1 = \frac{E_1 A_1}{\ell h}$$

$$(C_{1122})_1 = (C_{1112})_1 = (C_{2222})_1 = (C_{2212})_1 = (C_{1212})_1 = 0$$

$$(C_{1111})_2 = (C_{1122})_2 = (C_{1112})_2 = (C_{2212})_2 = (C_{1212})_2 = 0$$

$$(C_{2222})_2 = \frac{E_2 A_2}{\ell h}$$

$$(C_{1111})_3 = \frac{\sqrt{2}}{8}\frac{E_3 A_3}{\ell h} \quad ; \quad (C_{1122})_3 = \frac{\sqrt{2}}{8}\frac{E_3 A_3}{\ell h}$$

$$(C_{1112})_3 = -\frac{\sqrt{2}}{8}\frac{E_3 A_3}{\ell h} \quad ; \quad (C_{2222})_3 = \frac{\sqrt{2}}{8}\frac{E_3 A_3}{\ell h}$$

$$(C_{2212})_3 = \frac{\sqrt{2}}{8}\frac{E_3 A_3}{\ell h} \quad ; \quad (C_{1212})_3 = \frac{\sqrt{2}}{8}\frac{E_3 A_3}{\ell h}$$

$$(C_{1111})_4 = \frac{\sqrt{2}}{8}\frac{E_4 A_4}{\ell h} \quad ; \quad (C_{1122})_4 = \frac{\sqrt{2}}{8}\frac{E_4 A_4}{\ell h}$$

$$(C_{1112})_4 = -\frac{\sqrt{2}}{8}\frac{E_4 A_4}{\ell h} \quad ; \quad (C_{2222})_4 = \frac{\sqrt{2}}{8}\frac{E_4 A_4}{\ell h}$$

$$(C_{2212})_4 = -\frac{\sqrt{2}}{8}\frac{E_4 A_4}{\ell h} \quad ; \quad (C_{1212})_4 = \frac{\sqrt{2}}{8}\frac{E_4 A_4}{\ell h} \qquad (13)$$

When Eqs. (13) are substituted into Eqs. (9), the equivalent elastic continuum properties obtained are

$$C_{1111} = \frac{1}{\ell h}\left[E_1A_1 + \frac{\sqrt{2}}{8}(E_3A_3 + E_4A_4)\right]$$

$$C_{1122} = \frac{\sqrt{2}}{8\ell h}(E_3A_3 - E_4A_4)$$

$$C_{1112} = \frac{\sqrt{2}}{8\ell h}(E_3A_3 - E_4A_4)$$

$$C_{2222} = \frac{1}{\ell h}\left[E_2A_2 + \frac{\sqrt{2}}{8}(E_3A_3 + E_4A_4)\right]$$

$$C_{2212} = \frac{\sqrt{2}}{8\ell h}(E_3A_3 - E_4A_4) \qquad (14)$$

and the effective mass density is

$$\rho_0 = \frac{1}{\ell h}\left[\rho_1A_1 + \rho_2A_2 + \frac{\sqrt{2}}{2}(\rho_3A_3 + \rho_4A_4)\right] \qquad (15)$$

This example problem demonstrates the simplicity with which the equivalent continuum effective properties can be derived. The method shall now be applied to a three-dimensional truss.

2. A Three-Dimensional Problem - Tetrahedral Truss

A sample tetrahedral truss is shown in Fig. 3. It consists of two parallel layers of equilateral triangular meshes connected by bracing bars. The two triangular parallel layers form 0°, $\pm 60^\circ$ arrangement of the member orientation. The geometric and material properties of the truss members are summarized in Table 1.

If h is the height of the truss, ℓ is the length of the members in the top and bottom layers, and d is the length of bracing bars one can write.

$$d = \sqrt{h^2 + \frac{\ell^2}{3}} \tag{16}$$

A repeating element of this truss is shown in Fig. 4. Six sets of parallel members are identified by numbers 1 through 6. The direction cosines for these six sets are given in Table 2.

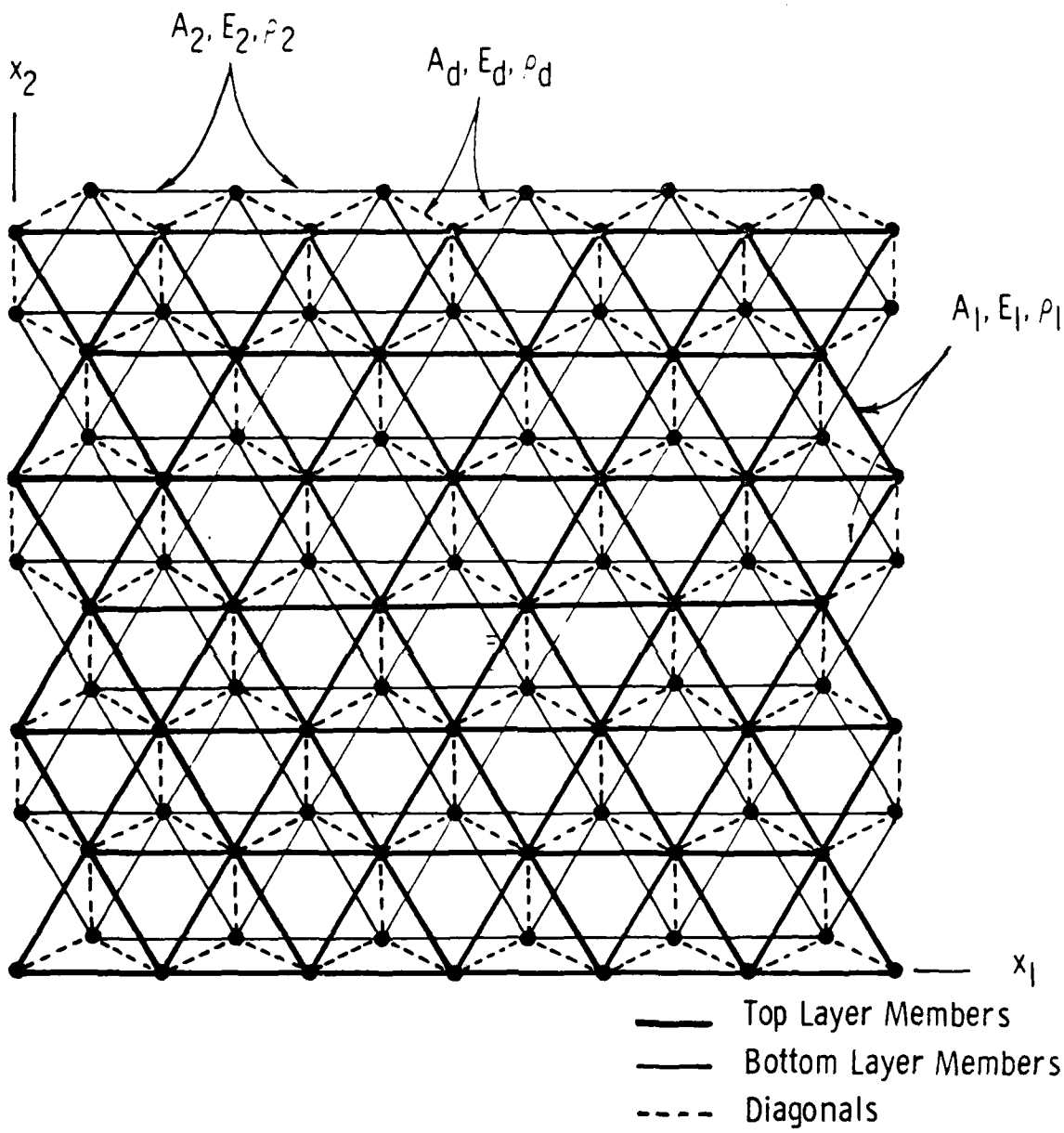

Fig. 3. Tetrahedral Truss

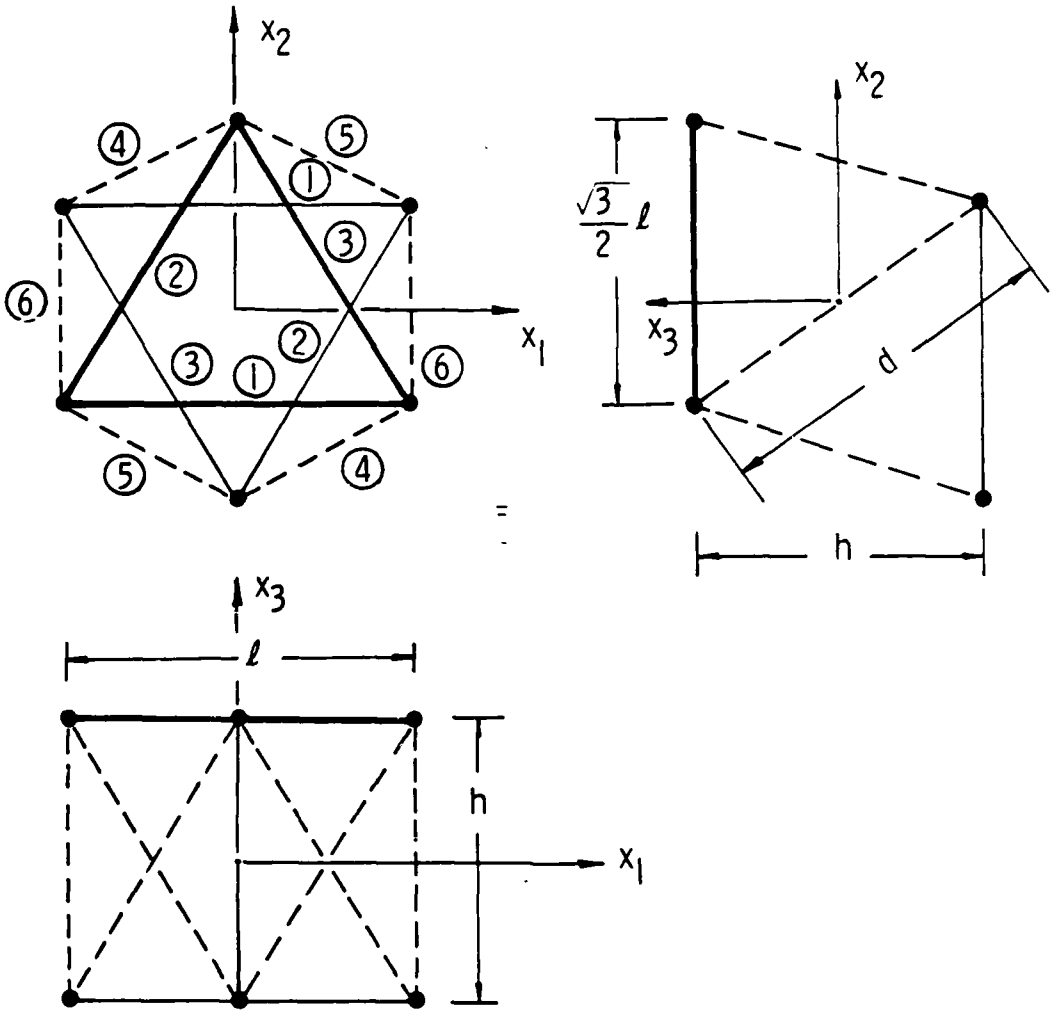

Fig. 4. Repeating Element of Tetrahedral Truss

Table 1. Geometric and Material Properties of the Tetrahedral Truss

	Cross-Sectional Area	Modulus of Elasticity	Mass Density	Length	Symbol
Top Layer Bars	A_1	E_1	ρ_1	ℓ	———
Bottom Layer Bars	A_2	E_2	ρ_2	ℓ	———
Bracing Bars	A_d	E_d	ρ_d	d	------

Table 2. Direction Cosines for Parallel Member Sets

Set Number	Direction Cosines		
	β_{11}	β_{21}	β_{31}
1	1	0	0
2	1/2	$\sqrt{3}$ /2	0
3	-1/2	$\sqrt{3}$ /2	0
4	ℓ/2d	$\sqrt{3}\ \ell$/6d	h/d
5	-ℓ/2d	$\sqrt{3}\ \ell$/6d	h/d
6	0	$\sqrt{3}\ \ell$/3d	h/d

Following the example problem discussed earlier, the unidirectional effective properties for the members in the top and bottom layers of the tetrahedral truss can be determined easily. The arrangement of the members in the present case is 0°, $\pm 60^{\circ}$. Table 3 lists the effective unidirectional properties of the three sets of the members in the top and bottom layers of the truss.

Table 3. Unidirectional Properties of the Members in the Top and Bottom Layers

Parallel Member Set Number	Effective Unidirectional Properties			
	Top Layer		Bottom Layer	
	Elastic	Mass	Elastic	Mass
1, 2, and 3	$\frac{2\sqrt{3}}{3}\ \frac{E_1 A_1}{\ell h}$	$\frac{2\sqrt{3}}{3}\ \frac{\rho_1 A_1}{\ell h}$	$\frac{2\sqrt{3}}{3}\ \frac{E_2 A_2}{\ell h}$	$\frac{2\sqrt{3}}{3}\ \frac{\rho_2 A_2}{\ell h}$

The effective unidirectional properties for the bracing members are determined next. A projection of the tetrahedral truss on a plane perpendicular to the parallel member Set 4 (see Fig. 4) is shown in Fig. 5. In this figure, bold dots represent the members of Set 4, whereas the effective area occupied by each member is shaded. Unidirectional effective elastic and mass properties for the Set 4 members are now computed by smearing the stiffness of each member over the effective area. Thus

$$\text{effective stiffness} = \frac{2\sqrt{3}}{3}\ \frac{d}{h\ell^2} E_d A_d$$

$$\text{effective mass} = \frac{2\sqrt{3}}{3}\ \frac{d}{h\ell^2} \rho_d A_d \qquad (17)$$

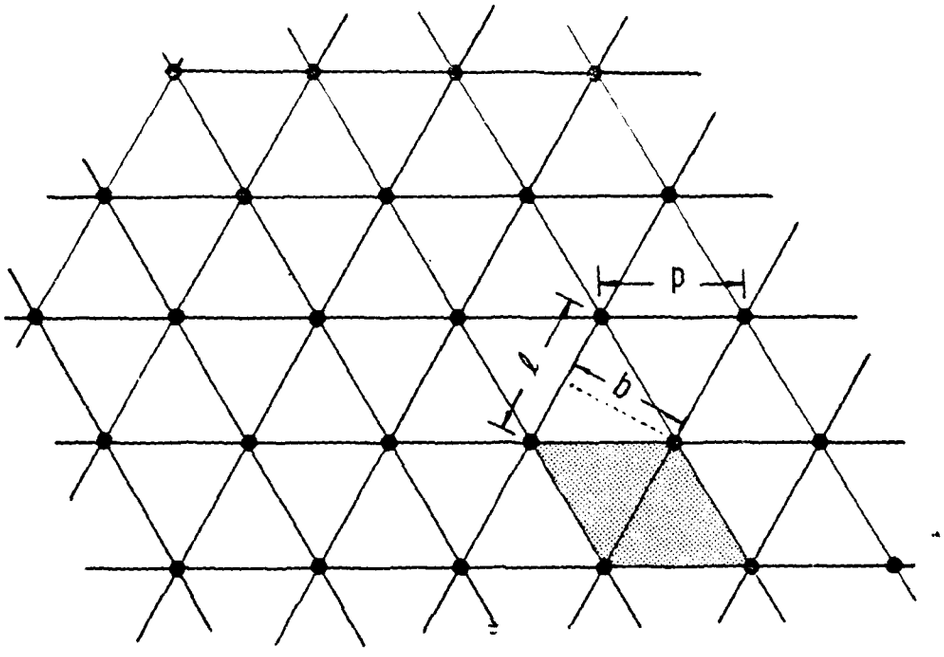

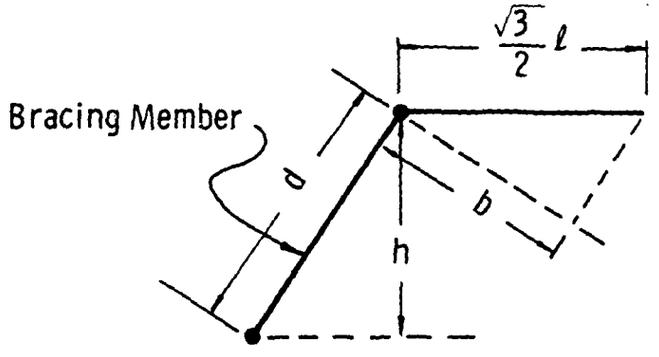

$$b = \frac{\sqrt{3}}{2}\,\frac{\ell h}{d}$$

Effective Area = $b\ell$

Fig. 5. Effective Area for Bracing Members

Equations (6), (9), and (10) are now used for deriving the elastic and mass properties of an equivalent continuum model. For the purpose of illustration, expression for the elastic constant C_{1111} is derived in detail. From Eq. (6), using Tables 2 and 3 and Eq. (17)

$$(C_{1111})_1 = (\beta_{11})_1^4 (C'_{1111})_1 = \frac{2\sqrt{3}}{3} \frac{E_1 A_1}{\ell h} + \frac{2\sqrt{3}}{3} \frac{E_2 A_2}{\ell h}$$

$$(C_{1111})_2 = (\beta_{11})_2^4 (C'_{1111})_2 = \frac{\sqrt{3}}{24} \frac{E_1 A_1}{\ell h} + \frac{\sqrt{3}}{24} \frac{E_2 A_2}{\ell h}$$

$$(C_{1111})_3 = (\beta_{11})_3^4 (C'_{1111})_3 = \frac{\sqrt{3}}{24} \frac{E_1 A_1}{\ell h} + \frac{\sqrt{3}}{24} \frac{E_2 A_2}{\ell h}$$

$$(C_{1111})_4 = (\beta_{11})_4^4 (C'_{1111})_4 = \frac{\sqrt{3}}{24} \frac{E_d A_d}{\ell h} \frac{\ell^3}{d^3}$$

$$(C_{1111})_5 = (\beta_{11})_5^4 (C'_{1111})_5 = \frac{\sqrt{3}}{24} \frac{E_d A_d}{\ell h} \frac{\ell^3}{d^3}$$

$$(C_{1111})_6 = (\beta_{11})_6^4 (C'_{1111})_6 = 0$$

Equation (9) yields

$$C_{1111} = \sum_{m=1}^{6} (C'_{1111})_m$$

or

$$C_{1111} = \frac{3\sqrt{3}}{4\ell h} \left(E_1 A_1 + E_2 A_2 + \frac{1}{9} \frac{\ell^3}{d^3} E_d A_d \right)$$

Similarly, other C_{ijkl}'s can be derived:

$$C_{1122} = \frac{\sqrt{3}}{4\ell h}\left(E_1A_1 + E_2A_2 + \frac{1}{9}\frac{\ell^3}{d^3}E_dA_d\right)$$

$$C_{1133} = \frac{\sqrt{3}}{3}\frac{h}{d^3}E_dA_d$$

$$C_{1123} = \frac{1}{6}\frac{\ell}{d^3}E_dA_d$$

$$C_{1131} = 0 \qquad C_{1112} = 0$$

$$C_{2222} = \frac{3\sqrt{3}}{4\ell h}\left(E_1A_1 + E_2A_2 + \frac{1}{9}\frac{\ell^3}{d^3}E_dA_d\right)$$

$$C_{2233} = \frac{\sqrt{3}}{3}\frac{h}{d^3}E_dA_d$$

$$C_{2223} = -\frac{1}{6}\frac{\ell}{d^3}E_dA_d$$

$$C_{2231} = 0 \qquad C_{2212} = 0$$

$$C_{3333} = 2\sqrt{3}\frac{h^3}{\ell^2 d^3}E_dA_d$$

$$C_{3323} = 0 \qquad C_{3331} = 0 \qquad C_{3312} = 0$$

$$C_{2323} = \frac{\sqrt{3}}{3}\frac{h}{d^3}E_dA_d$$

$$C_{2331} = 0 \qquad C_{2312} = 0$$

$$C_{3131} = \frac{\sqrt{3}}{3}\frac{h}{d^3}E_dA_d$$

$$C_{3112} = \frac{1}{6}\frac{\ell}{d^3}E_dA_d$$

$$C_{1212} = \frac{\sqrt{3}}{4\ell h}\left(E_1A_1 + E_2A_2 + \frac{1}{9}\frac{\ell^3}{d^3}E_dA_d\right) \qquad (18)$$

and the equivalent mass density is given by

$$\rho_0 = \frac{2\sqrt{3}}{\ell h} \left(\rho_1 A_1 + \rho_2 A_2 + \frac{d}{\ell} \rho_d A_d \right) \tag{19}$$

This completes the methodology for obtaining the equivalent elastic and mass properties for the continuum in terms of the geometric and material properties of a given tetrahedral truss.

In order to solve the continuum problem for predicting the structural response of the original truss, the governing field equations are (Ref. 27):

Equations of Motion

$$\frac{\partial \sigma_{ij}}{\partial x_j} + F_i = \rho_0 \frac{\partial^2 u_i}{\partial t^2} \tag{20}$$

Constitutive Equations

$$\sigma_{ij} = C_{ijk\ell} \epsilon_{k\ell} \qquad i,j,k,\ell = 1,2,3 \tag{21}$$

---

[27]Fung, Y.C., Foundations of Solid Mechanics, Prentice-Hall, Inc., Englewood Cliffs, NJ, 1965.

Strain-Displacement Relations

$$\epsilon_{ij} = \frac{1}{2}\left(\frac{\partial u_j}{\partial x_i} + \frac{\partial u_i}{\partial x_j}\right) \tag{22}$$

where F_i are the body forces and u_i are the displacement components. The problem in this form is so wrought with mathematical complexities that a general solution is almost impossible. However, it is often possible to make the problem tractable and obtain a reasonable solution through certain judicious assumptions.

III. SOLUTION OF THE CONTINUUM MODEL

The mathematical difficulties involved in determining solutions for the equivalent continuum model, derived in Section II, may be circumvented by making some simplified kinematic assumptions. For example, in the case of a tetrahedral truss representing a hypothetical large space platform, its equivalent continuum model can be viewed as a plate (Ref. 28). This is precisely the approach adopted in the present study.

Since the displacement components vary linearly along the members of the truss, it is assumed that the displacement components u_1, u_2, and u_3 of the equivalent continuum plate model vary linearly with the x_3 coordinate, i.e.

$$\begin{aligned} u_1 &= u_1^0 + x_3 \varphi_1 \\ u_2 &= u_2^0 + x_3 \varphi_2 \\ u_3 &= u_3^0 + x_3 \epsilon_{33}^0 \end{aligned} \tag{23}$$

where, as shown in Fig. 6, u_1^0, u_2^0, and u_3^0 are the mid-surface displacement components (at $x_3 = 0$), φ_1 and φ_2 are the rotation components, and ϵ_{33}^0 is the transverse normal strain. The mid-surface displacements, the rotation components, and the transverse normal strain are all assumed independent of the x_3 coordinate.

---

[28] Szilard, R., Theory and Analysis of Plates, Prentice-Hall, Inc., Englewood Cliffs, NJ, 1974.

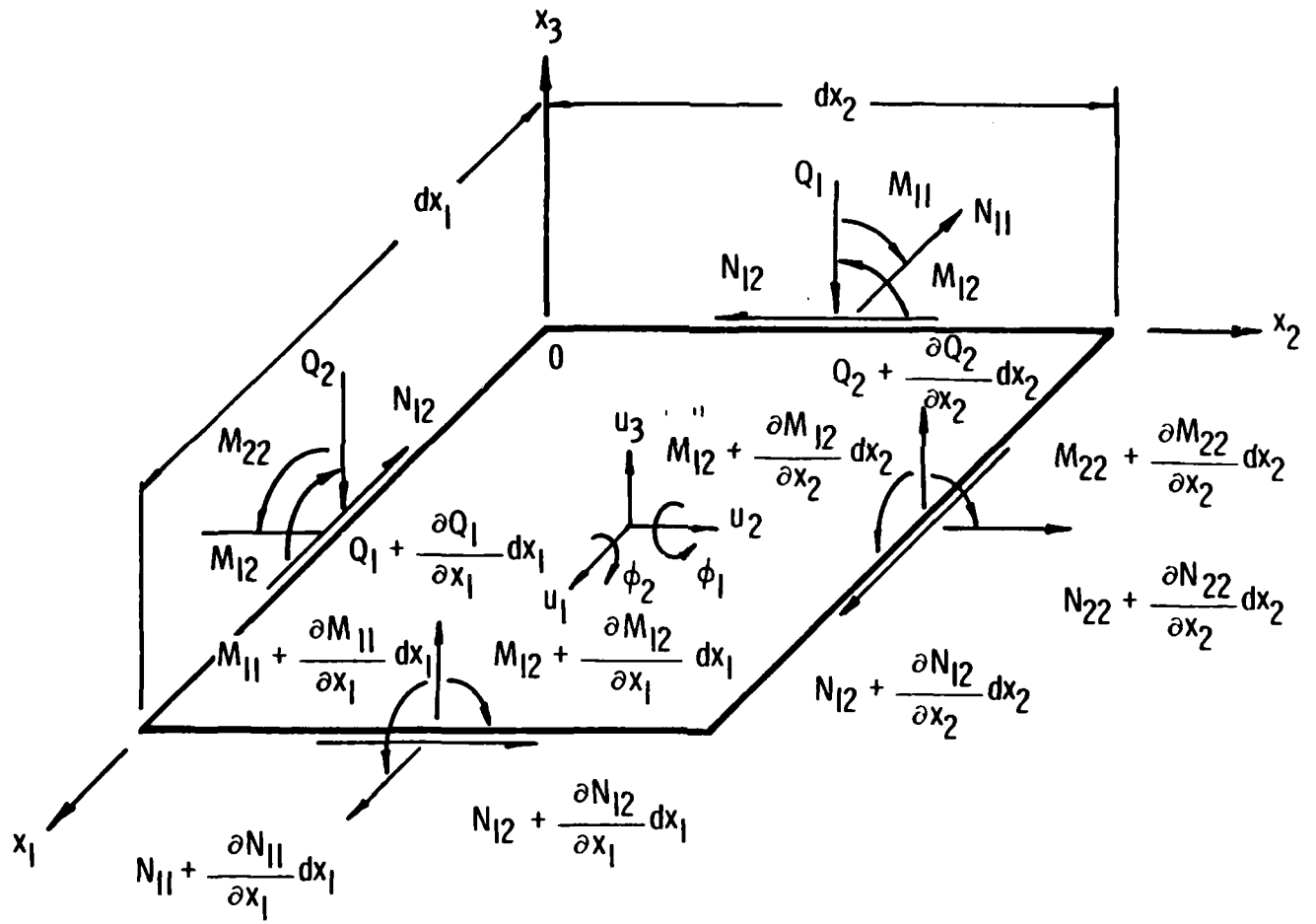

Fig. 6. Continuum Plate Model

As a consequence of this displacement field assumption, the strain components are

$$\epsilon_{11} = \frac{\partial u_1^0}{\partial x_1} + x_3 \frac{\partial \varphi_1}{\partial x_1}$$

$$\epsilon_{22} = \frac{\partial u_2^0}{\partial x_2} + x_3 \frac{\partial \varphi_2}{\partial x_2}$$

$$\epsilon_{12} = \frac{1}{2}\left(\frac{\partial u_2^0}{\partial x_1} + \frac{\partial u_1^0}{\partial x_2}\right) + \frac{1}{2} x_3 \left(\frac{\partial \varphi_2}{\partial x_1} + \frac{\partial \varphi_1}{\partial x_2}\right)$$

$$\epsilon_{33} = \epsilon_{33}^0$$

$$\epsilon_{23} = \frac{1}{2}\left(\frac{\partial u_3^0}{\partial x_2} + \varphi_2\right) + \frac{1}{2} x_3 \frac{\partial \epsilon_{33}^0}{\partial x_2}$$

$$\epsilon_{31} = \frac{1}{2}\left(\frac{\partial u_3^0}{\partial x_1} + \varphi_1\right) + \frac{1}{2} x_3 \frac{\partial \epsilon_{33}^0}{\partial x_1} \qquad (24)$$

The stress and moment resultants for the equivalent continuum plate are defined as follows:

Stress Resultants

$$N_{\alpha\beta} = \int_{-h/2}^{h/2} \sigma_{\alpha\beta}\, dx_3 \qquad \alpha, \beta = 1,2$$

$$N_{33} = \int_{-h/2}^{h/2} \sigma_{33}\, dx_3$$

$$Q_\alpha = \int_{-h/2}^{h/2} \sigma_{\alpha 3}\, dx_3 \qquad (25)$$

Moment Resultants

$$M_{\alpha\beta} = \int_{-h/2}^{h/2} \sigma_{\alpha\beta}\, x_3\, dx_3 \tag{26}$$

and

$$M_{\alpha} = \int_{-h/2}^{h/2} \sigma_{\alpha 3}\, x_3\, dx_3 \tag{27}$$

The equivalent stiffnesses (viz., extensional, coupling, and bending), for the continuum model are as follows:

Extensional Stiffness

$$A_{ijk\ell} = \int_{-h/2}^{h/2} C_{ijk\ell}\, dx_3 \tag{28}$$

Coupling Stiffness

$$B_{ijk\ell} = \int_{-h/2}^{h/2} C_{ijk\ell}\, x_3\, dx_3 \tag{29}$$

Bending Stiffness

$$D_{ijk\ell} = \int_{-h/2}^{h/2} C_{ijk\ell}\, x_3^2\, dx_3 \tag{30}$$

The relationships between the stress/moment resultants and the mid-surface strains are

$$N_{\alpha\beta} = A_{\alpha\beta\xi\eta}\,\epsilon^0_{\xi\eta} + A_{\alpha\beta 33}\epsilon^0_{33} + B_{\alpha\beta\xi\eta}\,\kappa_{\xi\eta}$$

$$N_{33} = A_{33\xi\eta}\,\epsilon^0_{\xi\eta} + A_{3333}\epsilon^0_{33} + B_{33\xi\eta}\,\kappa_{\xi\eta} \qquad (31)$$

$$Q_\alpha = 2A_{\alpha 3\xi 3}\,\epsilon^0_{\xi 3} + B_{\alpha 3\xi 3}\,\frac{\partial \epsilon^0_{33}}{\partial x_\xi}$$

$$M_{\alpha\beta} = B_{\alpha\beta\xi\eta}\,\epsilon^0_{\xi\eta} + B_{\alpha\beta 33}\epsilon^0_{33} + D_{\alpha\beta\xi\eta}\,\kappa_{\xi\eta}$$

$$M_\alpha = B_{\alpha 3\xi 3}\epsilon^0_{\xi 3} + D_{\alpha 3\xi 3}\,\frac{\partial \epsilon^0_{33}}{\partial x_\xi} \qquad (32)$$

where α, β, ξ and η = 1,2, and 3

$$\epsilon^0_{\alpha\beta} = \frac{1}{2}\left(\frac{\partial u^0_\beta}{\partial x_\alpha} + \frac{\partial u^0_\alpha}{\partial x_\beta}\right)$$

$$\epsilon^0_{\xi 3} = \frac{1}{2}\left(\frac{\partial u^0_3}{\partial x_\xi} + \varphi_\xi\right)$$

$$\kappa_{\alpha\beta} = \frac{1}{2}\left(\frac{\partial \varphi_\beta}{\partial x_\alpha} + \frac{\partial \varphi_\alpha}{\partial x_\beta}\right) \qquad (33)$$

The equations of motion for the equivalent continuum plate model are [using Eqs. (20)]

$$\frac{\partial N_{11}}{\partial x_1} + \frac{\partial N_{12}}{\partial x_2} + q_1 = \bar{\rho}_0 \frac{\partial^2 u_1^0}{\partial t^2} + \bar{\rho}_1 \frac{\partial^2 \varphi_1}{\partial t^2}$$

$$\frac{\partial N_{12}}{\partial x_1} + \frac{\partial N_{22}}{\partial x_2} + q_2 = \bar{\rho}_0 \frac{\partial^2 u_2^0}{\partial t^2} + \bar{\rho}_1 \frac{\partial^2 \varphi_2}{\partial t^2}$$

$$\frac{\partial Q_1}{\partial x_1} + \frac{\partial Q_2}{\partial x_2} + q_3 = \bar{\rho}_0 \frac{\partial^2 u_3^0}{\partial t^2} + \bar{\rho}_1 \frac{\partial^2 \epsilon_{33}^0}{\partial t^2}$$

$$\frac{\partial M_{11}}{\partial x_1} + \frac{\partial M_{12}}{\partial x_2} - Q_1 + M_1 = \bar{\rho}_1 \frac{\partial^2 u_1^0}{\partial t^2} + \bar{\rho}_2 \frac{\partial^2 \varphi_1}{\partial t^2}$$

$$\frac{\partial M_{12}}{\partial x_1} + \frac{\partial M_{22}}{\partial x_2} - Q_2 + M_2 = \bar{\rho}_1 \frac{\partial^2 u_2^0}{\partial t^2} + \bar{\rho}_2 \frac{\partial^2 \varphi_2}{\partial t^2}$$

$$\frac{\partial M_1}{\partial x_1} + \frac{\partial M_2}{\partial x_2} - N_{33} + M_3 = \bar{\rho}_1 \frac{\partial^2 u_3^0}{\partial t^2} + \bar{\rho}_2 \frac{\partial^2 \epsilon_{33}^0}{\partial t^2} \qquad (34)$$

where q_1, q_2, and q_3 are the external load components and M_1, M_2, and M_3 are the external moment components in the x_1, x_2, and x_3 directions, respectively.

Also

$$\bar{\rho}_0 = \int_{-h/2}^{h/2} \rho_0 \, dx_3$$

$$\bar{\rho}_1 = \int_{-h/2}^{h/2} \rho_0 \, x_3 \, dx_3$$

and

$$\bar{\rho}_2 = \int_{-h/2}^{h/2} \rho_0 \, x_3^2 \, dx_3 \qquad (35)$$

An example poblem is discussed in Section IV.

IV. EXAMPLE PROBLEM

A. EQUIVALENT STIFFNESSES

In order to assess the accuracy of using the equivalent continuum model, the methodology was applied to a hypothetical space platform (Fig. 3) composed of an assembly of tetrahedral trusses. The extensional, coupling, and bending stiffnesses are determined from Eqs. (28) through (30) following the procedure given by Heki (Ref. 29):

Extensional Stiffness

$$A_{1111} = \frac{3\sqrt{3}}{4\ell}\left(E_1A_1 + E_2A_2 + \frac{1}{9}\frac{\ell^3}{d^3}E_dA_d\right)$$

$$A_{1122} = \frac{\sqrt{3}}{4\ell}\left(E_1A_1 + E_2A_2 + \frac{1}{9}\frac{\ell^3}{d^3}E_dA_d\right)$$

$$A_{1133} = \frac{\sqrt{3}}{3}\frac{h^2}{d^3}E_dA_d$$

$$A_{1123} = \frac{1}{6}\frac{\ell h}{d^3}E_dA_d$$

$$A_{1131} = 0 \qquad A_{1112} = 0$$

$$A_{2222} = \frac{3\sqrt{3}}{4\ell}\left(E_1A_1 + E_2A_2 + \frac{1}{9}\frac{\ell^3}{d^3}E_dA_d\right)$$

---

[29]Heki, K., "On the Effective Rigidities of Lattice Plates," Recent Researches of Structural Mechanics, Tokyo, 1968.

$$A_{2233} = \frac{\sqrt{3}}{3} \frac{h^2}{d^3} E_d A_d$$

$$A_{2223} = -\frac{1}{6} \frac{\ell h}{d^3} E_d A_d$$

$$A_{2231} = 0 \qquad A_{2212} = 0$$

$$A_{3333} = 2\sqrt{3} \frac{h^3}{\ell^2 d^3} E_d A_d$$

$$A_{3323} = 0 \qquad A_{3312} = 0 \qquad A_{3331} = 0$$

$$A_{2323} = \frac{\sqrt{3}}{3} \frac{h^2}{d^3} E_d A_d$$

$$A_{2331} = 0 \qquad A_{2312} = 0$$

$$A_{3131} = \frac{\sqrt{3}}{3} \frac{h^2}{d^3} E_d A_d$$

$$A_{3112} = \frac{1}{6} \frac{\ell h}{d^3} E_d A_d$$

$$A_{1212} = \frac{\sqrt{3}}{4\ell} \left(E_1 A_1 + E_2 A_2 + \frac{1}{9} \frac{\ell^3}{d^3} E_d A_d \right) \qquad (36)$$

Coupling Stiffness

$$B_{1111} = \frac{3\sqrt{3}}{8}\frac{h}{\ell}(E_1A_1 - E_2A_2)$$

$$B_{1122} = \frac{\sqrt{3}}{8}\frac{h}{\ell}(E_1A_1 - E_2A_2)$$

$$B_{1133} = B_{1123} = B_{1131} = B_{1112} = 0$$

$$B_{2222} = \frac{3\sqrt{3}}{8}\frac{h}{\ell}(E_1A_1 - E_2A_2)$$

$$B_{2233} = B_{2223} = B_{2231} = B_{2212} = 0$$

$$B_{3333} = B_{3323} = B_{3331} = B_{3312} = 0$$

$$B_{2323} = B_{2331} = B_{2312} = 0$$

$$B_{3131} = B_{3112} = 0$$

$$B_{1212} = \frac{\sqrt{3}}{8\ell}(E_1A_1 - E_2A_2) \qquad (37)$$

Bending Stiffnesses

$$D_{1111} = \frac{3\sqrt{3}}{16}\frac{h^2}{\ell}(E_1A_1 + E_2A_2)$$

$$D_{1122} = \frac{\sqrt{3}}{16}\frac{h^2}{\ell}(E_1A_1 + E_2A_2)$$

$$D_{2222} = \frac{3\sqrt{3}}{16}\frac{h^2}{\ell}(E_1A_1 + E_2A_2)$$

$$D_{1212} = \frac{\sqrt{3}}{16}\frac{h^2}{\ell}(E_1A_1 + E_2A_2) \qquad (38)$$

The density parameters for the equivalent continuum model are obtained from Eqs. (19) and (35):

$$\bar{\rho}_0 = \frac{2\sqrt{3}}{\ell}\left(\rho_1 A_1 + \rho_2 A_2 + \frac{d}{\ell}\rho_d A_d\right)$$

$$\bar{\rho}_1 = \frac{\sqrt{3}\,h}{\ell}\left(\rho_1 A_1 - \rho_2 A_2\right)$$

$$\bar{\rho}_2 = \frac{\sqrt{3}}{2}\frac{h^2}{\ell}\left(\rho_1 A_1 + \rho_2 A_2 + \frac{1}{3}\frac{d}{\ell}\rho_d A_d\right) \tag{39}$$

With the help of Eqs. (31) through (33), and Eqs. (36) through (38), the equations of motion (34) are rewritten in terms of the displacements and rotation components as follows:

$$A_{1111}\frac{\partial^2 u_1^0}{\partial x_1^2} + A_{1212}\frac{\partial^2 u_1^0}{\partial x_2^2} + (A_{1122} + A_{1212})\frac{\partial^2 u_2^0}{\partial x_1 \partial x_2} + A_{1133}\frac{\partial \epsilon_{33}^0}{\partial x_1}$$

$$+ B_{1111}\frac{\partial^2 \varphi_1}{\partial x_1^2} + B_{1212}\frac{\partial^2 \varphi_1}{\partial x_2^2} + (B_{1122} + B_{1212})\frac{\partial^2 \varphi_2}{\partial x_1 \partial x_2}$$

$$+ q_1 = \bar{\rho}_0\frac{\partial^2 u_1^0}{\partial t^2} + \bar{\rho}_1\frac{\partial^2 \varphi_1}{\partial t^2} \tag{40}$$

$$(A_{1212} + A_{1122}) \frac{\partial^2 u_1^0}{\partial x_1 \partial x_2} + A_{1212} \frac{\partial^2 u_2^0}{\partial x_1^2} + A_{2222} \frac{\partial^2 u_2^0}{\partial x_2^2} + A_{2233} \frac{\partial \epsilon_{33}^0}{\partial x_2}$$

$$+ (B_{1212} + B_{1122}) \frac{\partial^2 \varphi_1}{\partial x_1 \partial x_2} + B_{1212} \frac{\partial^2 \varphi_2}{\partial x_1^2} + B_{2222} \frac{\partial^2 \varphi_2}{\partial x_2^2}$$

$$+ q_2 = \bar{\rho}_0 \frac{\partial^2 u_2^0}{\partial t^2} + \bar{\rho}_1 \frac{\partial^2 \varphi_2}{\partial t^2} \tag{41}$$

$$A_{3131} \frac{\partial^2 u_3^0}{\partial x_1^2} + A_{2323} \frac{\partial^2 u_3^0}{\partial x_2^2} + A_{1313} \frac{\partial \varphi_1}{\partial x_1} + A_{2323} \frac{\partial \varphi_2}{\partial x_2}$$

$$+ q_3 = \bar{\rho}_0 \frac{\partial^2 u_3^0}{\partial t^2} + \bar{\rho}_1 \frac{\partial^2 \bar{\epsilon}_{33}^0}{\partial t^2} \tag{42}$$

$$B_{1111} \frac{\partial^2 u_1^0}{\partial x_1^2} + B_{1212} \frac{\partial^2 u_1^0}{\partial x_2^2} - (B_{1122} + B_{1212}) \frac{\partial^2 u_2^0}{\partial x_1 \partial x_2} + D_{1111} \frac{\partial^2 u_1^0}{\partial x_1^2}$$

$$+ D_{1212} \frac{\partial^2 \varphi_1}{\partial x_2^2} + (D_{1122} + D_{1212}) \frac{\partial^2 \varphi_2}{\partial x_1 \partial x_2} - A_{3131} \left(\frac{\partial u_3^0}{\partial x_1} + \varphi_1 \right)$$

$$+ M_1 = \bar{\rho}_1 \frac{\partial^2 u_1^0}{\partial t^2} + \bar{\rho}_2 \frac{\partial^2 \varphi_1}{\partial t^2} \tag{43}$$

$$(B_{1122} + B_{1212}) \frac{\partial^2 u_1^0}{\partial x_1 \partial x_2} + B_{1212} \frac{\partial^2 u_2^0}{\partial x_1^2} + B_{2222} \frac{\partial^2 u_2^0}{\partial x_2^2}$$

$$+ (D_{1122} + D_{1212}) \frac{\partial^2 \varphi_1}{\partial x_1 \partial x_2} + D_{1212} \frac{\partial^2 \varphi_2}{\partial x_1^2} + D_{2222} \frac{\partial^2 \varphi_2}{\partial x_2^2}$$

$$- A_{2323}\left(\frac{\partial u_3^0}{\partial x_2} + \varphi_2\right) + M_2 = \bar{\rho}_1 \frac{\partial^2 u_2^0}{\partial t^2} + \bar{\rho}_2 \frac{\partial^2 \varphi_2}{\partial t^2} \qquad (44)$$

$$- A_{1133} \frac{\partial^2 u_1^0}{\partial x_1} - A_{2233} \frac{\partial^2 u_2^0}{\partial x_2} - A_{3333} \epsilon_{33}^0 + M_3 = \bar{\rho}_1 \frac{\partial^2 u_3^0}{\partial t^2} + \bar{\rho}_2 \frac{\partial^2 \epsilon_{33}^0}{\partial t^2} \qquad (45)$$

In the present example problem, the cross-sectional areas of the members in the top and the bottom layers are assumed to be identical and all the members lengths are equal, i.e.

$$A_1 = A_2 = A$$

$$d = \ell$$

Also

$$E_1 = E_2 = E_d = E$$

$$\rho_1 = \rho_2 = \rho_d = \rho$$

The consequence of these assumptions is that $\bar{\rho}_1$ and all $B_{ijk\ell}$'s are zero.

Also from Eqs. (38)

$$D_{1111} = D_{2222} = D \text{ (say)}$$

and

$$D_{1122} = D_{1212} = D/3$$

The stiffness and mass properties of the equivalent continuum model are summarized in Table 4.

Table 4. Equivalent Continuum Model Properties

Extensional Stiffness	
$A_{1111} = A_{2222}$	$\frac{3\sqrt{3}}{4} \frac{E}{\ell} \left(2A + \frac{1}{9} A_d\right)$
$A_{1122} = A_{1212}$	$\frac{\sqrt{3}}{4} \frac{E}{\ell} \left(2A + \frac{1}{9} A_d\right)$
$A_{1133} = A_{2233} = A_{2323} = A_{3131}$	$\frac{2\sqrt{3}}{9} \frac{E}{\ell} A_d$
A_{3333}	$\frac{8\sqrt{3}}{9} \frac{E}{\ell} A_d$
$A_{1123} = -A_{2223} = A_{3112}$	$-\frac{\sqrt{6}}{18} \frac{E}{\ell} A_d$
Bending Stiffness	
$D_{1111} = D_{2222} = D$	$\frac{\sqrt{3}}{4} EA\ell$
$D_{1122} = D_{1212} = D/3$	$\frac{\sqrt{3}}{12} EA\ell$
Mass and Moment of Inertia	
$\bar{\rho}_0$	$2\sqrt{3} \frac{\rho}{\ell} (2A + A_d)$
$\bar{\rho}_2$	$\frac{\sqrt{3}}{3} \rho\ell \left(2A + \frac{1}{3} A_d\right)$

The equations of motion (40) through (45) now simplify as

$$A_{1111}\frac{\partial^2 u_1^0}{\partial x_1^2} + A_{1212}\frac{\partial^2 u_1^0}{\partial x_2^2} + 2A_{1212}\frac{\partial^2 u_2^0}{\partial x_1 \partial x_2} + A_{1133}\frac{\partial \epsilon_{33}^0}{\partial x_1} + q_1 = \bar{\rho}_0 \frac{\partial^2 u_1^0}{\partial t^2} \tag{46}$$

$$2A_{1212}\frac{\partial^2 u_1^0}{\partial x_1 \partial x_2} + A_{1212}\frac{\partial^2 u_2^0}{\partial x_1^2} + A_{1111}\frac{\partial^2 u_2^0}{\partial x_2^2} + A_{1133}\frac{\partial \epsilon_{33}^0}{\partial x_2} + q_2 = \bar{\rho}_0 \frac{\partial^2 u_2^0}{\partial t^2} \tag{47}$$

$$A_{3131}\left(\frac{\partial^2 u_3^0}{\partial x_1^2} + \frac{\partial^2 u_3^0}{\partial x_2^2}\right) + A_{3131}\left(\frac{\partial \varphi_1}{\partial x_1} + \frac{\partial \varphi_2}{\partial x_2}\right) + q_3 = \bar{\rho}_0 \frac{\partial^2 u_3^0}{\partial t^2} \tag{48}$$

$$D\frac{\partial^2 \varphi_1}{\partial x_1^2} + \frac{D}{3}\frac{\partial^2 \varphi_1}{\partial x_2^2} + \frac{2D}{3}\frac{\partial^2 \varphi_2}{\partial x_1 \partial x_2} - A_{3131}\left(\frac{\partial u_3^0}{\partial x_1} + \varphi_1\right) + M_1 = \bar{\rho}_2 \frac{\partial^2 \varphi_1}{\partial t^2} \tag{49}$$

$$\frac{2D}{3}\frac{\partial^2 \varphi_1}{\partial x_1 \partial x_2} + \frac{D}{3}\frac{\partial^2 \varphi_2}{\partial x_1^2} + D\frac{\partial^2 \varphi_2}{\partial x_2^2} - A_{3131}\left(\frac{\partial u_3^0}{\partial x_2} + \varphi_2\right) + M_2 = \bar{\rho}_2 \frac{\partial^2 \varphi_2}{\partial t^2} \tag{50}$$

$$A_{1133}\left(\frac{\partial u_1^0}{\partial x_1} + \frac{\partial u_2^0}{\partial x_2}\right) + A_{3333}\epsilon_{33}^0 + M_3 = \bar{\rho}_2 \frac{\partial^2 \epsilon_{33}^0}{\partial t^2} \tag{51}$$

The accuracy of the equivalent continuum model developed is illustrated by the following free vibration problem in which comparison of the natural frequencies obtained from the continuum model is made with those obtained directly from the actual truss structure solution. For the free vibration case

$$q_i \equiv 0 \qquad i = 1, 2, 3$$

and

$$M_i \equiv 0$$

Differentiating Eqs. (49) and (50) with respect to x_1 and x_2, respectively and adding them together yield

$$D\left(\frac{\partial^2\psi}{\partial x_1^2}+\frac{\partial^2\psi}{\partial x_2^2}\right)-A_{3131}\left(\frac{\partial^2 u_3^0}{\partial x_1^2}+\frac{\partial^2 u_3^0}{\partial x_2^2}\right)-A_{3131}\psi=\bar{\rho}_2\frac{\partial^2\psi}{\partial t^2} \tag{52}$$

where

$$\psi \equiv \frac{\partial\varphi_1}{\partial x_1}+\frac{\partial\varphi_2}{\partial x_2}$$

Equation (48) can be rewritten as

$$A_{3131}\left(\frac{\partial^2 u_3^0}{\partial x_1^2}+\frac{\partial^2 u_3^0}{\partial x_2^2}\right)+A_{3131}\psi=\bar{\rho}_0\frac{\partial^2 u_3^0}{\partial t^2} \tag{53}$$

or

$$\psi=\frac{\bar{\rho}_0}{A_{3131}}\frac{\partial^2 u_3^0}{\partial t^2}-\nabla^2 u_3^0 \tag{54}$$

where operator

$$\nabla^2=\frac{\partial^2}{\partial x_1^2}+\frac{\partial^2}{\partial x_2^2}$$

Substitution of ψ from Eq. (53) gives

$$\left(D\nabla^2-\bar{\rho}_2\frac{\partial^2}{\partial t^2}\right)\left(\nabla^2-\frac{\bar{\rho}_0}{A_{3131}}\frac{\partial^2}{\partial t^2}\right)u_3^0+\bar{\rho}_0\frac{\partial^2 u_3^0}{\partial t^2}=0 \tag{55}$$

Equation (55) includes the rotary inertia as well as transverse shear deformation terms.

If the rotary inertia terms are omitted from Eq. (55), it reduces to

$$D\left(\nabla^2 - \frac{\bar{\rho}_0}{A_{3131}}\frac{\partial^2}{\partial t^2}\right)\nabla^2 u_3^0 + \bar{\rho}_0\frac{\partial^2 u_3^0}{\partial t^2} = 0 \qquad (56)$$

If the transverse shear deformation is neglected, but the rotary inertia terms are retained, Eq. (55) reduces to

$$\left(D\nabla^2 - \bar{\rho}_2\frac{\partial^2}{\partial t^2}\right)\nabla^2 u_3^0 + \bar{\rho}_0\frac{\partial^2 u_3^0}{\partial t^2} = 0 \qquad (57)$$

Finally, if both the transverse shear deformation and rotary inertia terms are omitted, Eq. (55) reduces to the classical plate equation

$$D\nabla^4 u_3^0 + \bar{\rho}_0\frac{\partial^2 u_3^0}{\partial t^2} = 0 \qquad (58)$$

The solution of Eqs. (55), (56), (57), or (58) for appropriate boundary conditions shall yield the natural frequencies for the equivalent continuum model.

The significance of including the rotary inertia and transverse shear terms has been discussed by Reissner (Ref. 30), and Mindlin (Refs. 31, 32).

---

[30]Reissner, E., "The Effect of Transverse Shear Deformation on the Bending of Elastic Plates," Journal of Applied Mechanics, Vol. 12, June 1945.

[31]Mindlin, R. D., "Influence of Rotary Inertia and Shear on Flexural Motions of Isotropic, Elastic Plates," Journal of Applied Mechanics, Vol. 18, No. 1, March 1951.

[32]Mindlin, R. D., A. Schacknow, and H. Deresiewicz, "Flexural Vibrations of Rectangular Plates," Journal of Applied Mechanics, Vol. 23, No. 3, September 1956.

It is known that both effects serve to decrease the computed frequencies because of the increased inertia and flexibility of the system. In the present study, the natural frequencies are computed from Eqs. (55) through (58) and compared with those obtained from solving the original truss structure.

As a first example case, simply supported boundary conditions are assumed. It is possible to obtain the continuum model closed form solution for such boundary conditions. These boundary conditions may be stated (see Fig. 7)

$$u_3^0 = 0 \quad , \quad M_{11} = 0 \quad \text{at} \quad x_1 = 0 \quad \text{and} \quad x_1 = a$$

$$u_3^0 = 0 \quad , \quad M_{22} = 0 \quad \text{at} \quad x_2 = 0 \quad \text{and} \quad x_2 = b$$

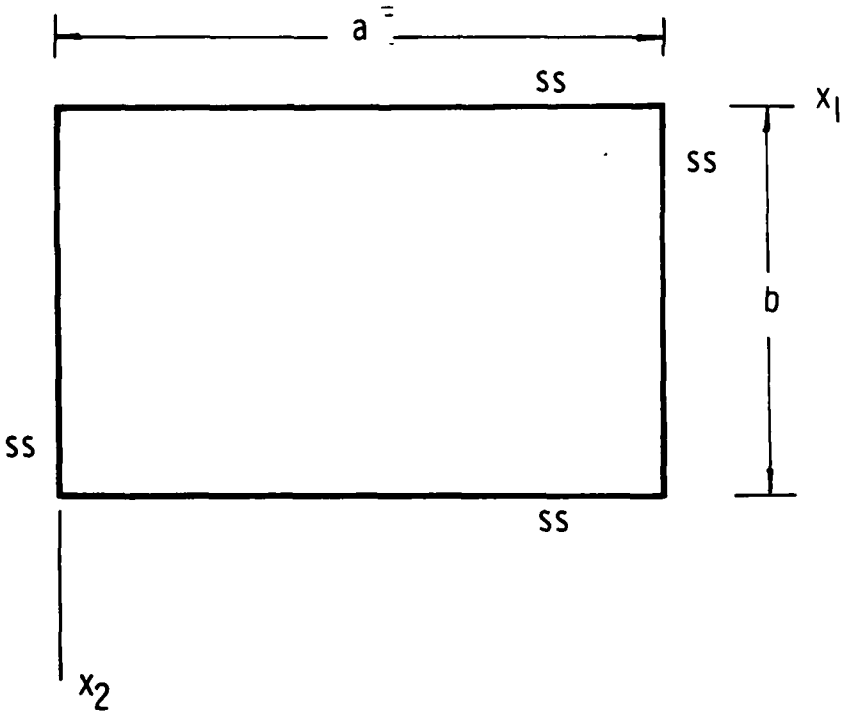

Fig. 7. Simply Supported Plate

Assuming displacement u_3^0 as

$$u_3^0 = \Lambda \sin \frac{m\pi x_1}{a} \sin \frac{n\pi x_2}{b} e^{i\omega t} \tag{59}$$

where Λ is a constant, m and n are integers, and ω is circular frequency. It is clear that the boundary conditions are automatically satisfied by the displacement function. The frequency ω may now be determined by substituting u_3^0 into Eqs. (55) through (58).

Case 1. Rotary inertia and transverse shear terms included. The characteristic equation in this case, obtained from Eq. (55) is

$$\frac{\bar{\rho}_0 \bar{\rho}_2}{A_{3131}} \omega^4 - \left[\pi^2 \left(\frac{\bar{\rho}_0 D}{A_{3131}} + \rho_2 \right) \left(\frac{m^2}{a^2} + \frac{n^2}{b^2} \right) + \bar{\rho}_0 \right] \omega^2 + \pi^4 D \left(\frac{m^2}{a^2} + \frac{n^2}{b^2} \right)^2 = 0 \tag{60}$$

Case 2. Transverse shear term included, rotary inertia term omitted. The natural frequencies in this case, obtained from Eq. (56), are given by

$$\omega^2 = \frac{\pi^4 D}{\bar{\rho}_0} \frac{\left(\frac{m^2}{a^2} + \frac{n^2}{b^2} \right)^2}{\left[\frac{\pi^2 D}{A_{3131}} \left(\frac{m^2}{a^2} + \frac{n^2}{b^2} \right) + 1 \right]} \tag{61}$$

Case 3. Rotary inertia term included, transverse shear term omitted. In this case, the natural frequencies, obtained from Eq. (57), are given by

$$\omega^2 = \frac{\pi^4 D}{\bar{\rho}_0} \frac{\left(\frac{m^2}{a^2} + \frac{n^2}{b^2} \right)^2}{\left[\frac{\pi^2 \bar{\rho}_2}{\bar{\rho}_0} \left(\frac{m^2}{a^2} + \frac{n^2}{b^2} \right)^2 + 1 \right]} \tag{62}$$

Case 4. Classical plate solution. The natural frequencies in this case, obtained from Eq. (58), are given by

$$\omega^2 = \frac{\pi^4 D}{\bar{\rho}_0}\left(\frac{m^2}{a^2} + \frac{n^2}{b^2}\right)^2 \tag{63}$$

B. NUMERICAL RESULTS

The following geometric and material properties were assumed for the tetrahedral truss:

Case A

$A = A_d = 50 \times 10^{-6}\ m^2$

$\ell = 6\ m$

$\rho = 2768\ kg/m^3$

$E = 71.7 \times 10^6\ kPa$

Case B

$A = 50 \times 10^{-6}\ m^2$

$A_d = 2.5 \times 10^{-6}\ m^2$

$\ell = 6\ m$

$\rho = 2768\ kg/m^3$

$E = 71.7 \times 10^6\ kPa$

The natural frequencies for the tetrahedral truss with 6, 8, 12, and 18 repeating elements in each direction were computed using the NASTRAN computer program. Equations (60) through (63) are used for computing the natural frequencies of the equivalent continuum model. If N is the number of the repeating tetrahedral truss elements in each direction, plate dimensions a and b are given by

$$a = N\ell \qquad b = \frac{\sqrt{3}}{2} N\ell$$

The results are summarized in Tables 5 through 12 and in Figs. 8 through 15. The finite element solution of the truss is represented by FEM in the tables, whereas I through IV represent the continuum solutions with varying degrees of approximations. These are defined as follows:

I = Transverse shear and rotary inertia terms included
II = Transverse shear terms only included
III = Rotary inertia terms only included
IV = Classical plate solution

The undeformed shape of a truss with 12 repeating tetrahedral elements (orthographic view) is shown in Fig. 16, whereas its projections on the X-Z plane and the Y-Z plane are shown in Figs. 17 and 18, respectively. The corresponding views for the first four mode shapes of the same truss structure are shown in Figs. 19 through 30.

Table 5. Comparison of Natural Frequencies - First Mode

CASE A: $A_d = A$				
f_{11} \ N	6	8	12	18
FEM	13.67	8.86	4.51	2.18
I	13.26	8.28	4.03	1.88
II	13.44	8.37	4.06	1.88
III	16.94	9.69	4.36	1.95
IV	17.63	9.92	4.41	1.96

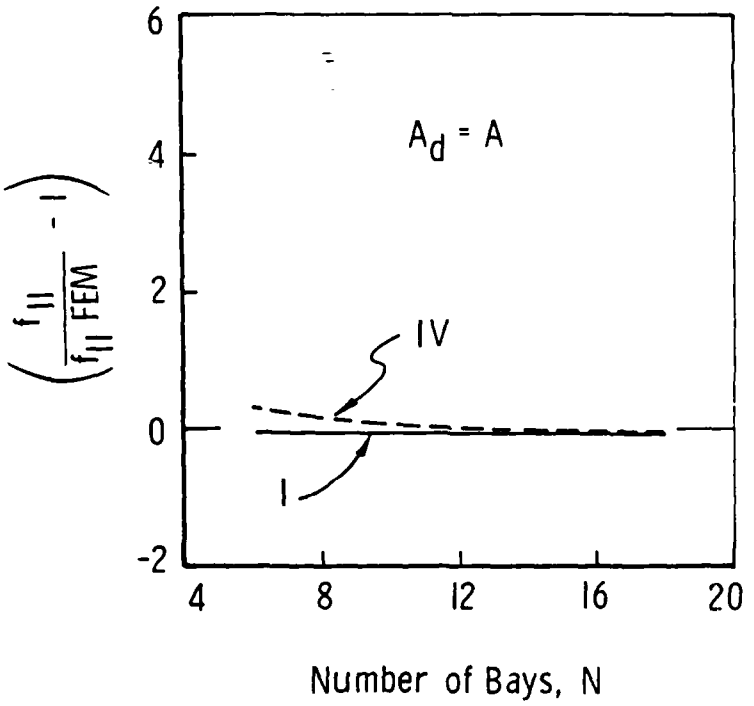

Fig. 8. Comparison of Natural Frequencies - First Mode

Table 6. Comparison of Natural Frequencies - Second Mode

CASE A: $A_d = A$				
f_{21} \ N	6	8	12	16
FEM	22.00	15.08	8.20	4.13
I	24.43	16.11	8.38	4.09
II	24.78	16.33	8.48	4.12
III	36.94	21.55	9.84	4.43
IV	40.29	22.67	10.07	4.48

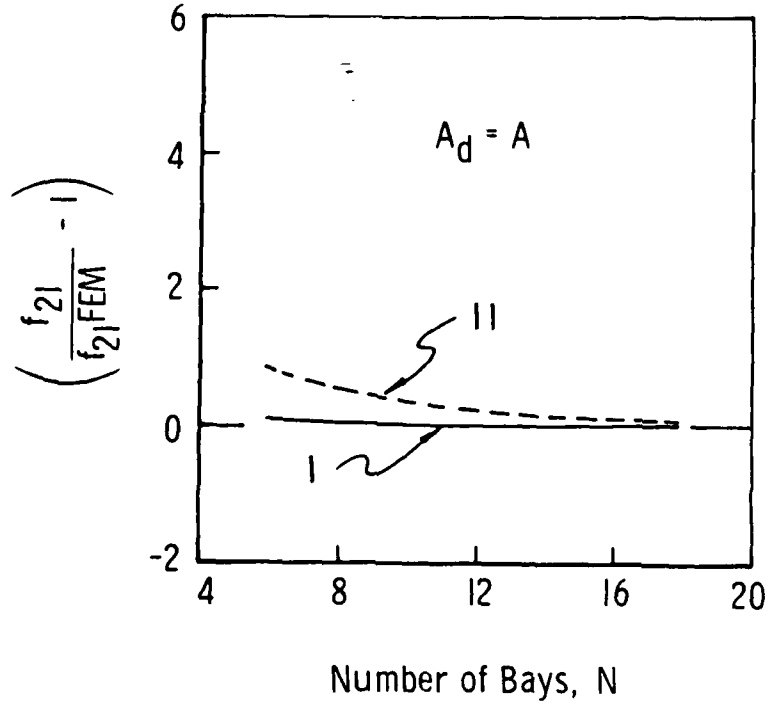

Fig. 9. Comparison of Natural Frequencies - Second Mode

Table 7. Comparison of Natural Frequencies - Third Mode

CASE A: $A_d = A$				
f_{12} \ N	6	8	12	18
FEM	24.60	17.06	9.36	4.76
I	27.47	18.30	9.68	4.78
II	27.84	18.58	9.81	4.82
III	43.23	25.36	11.64	5.25
IV	47.85	26.91	11.96	5.32

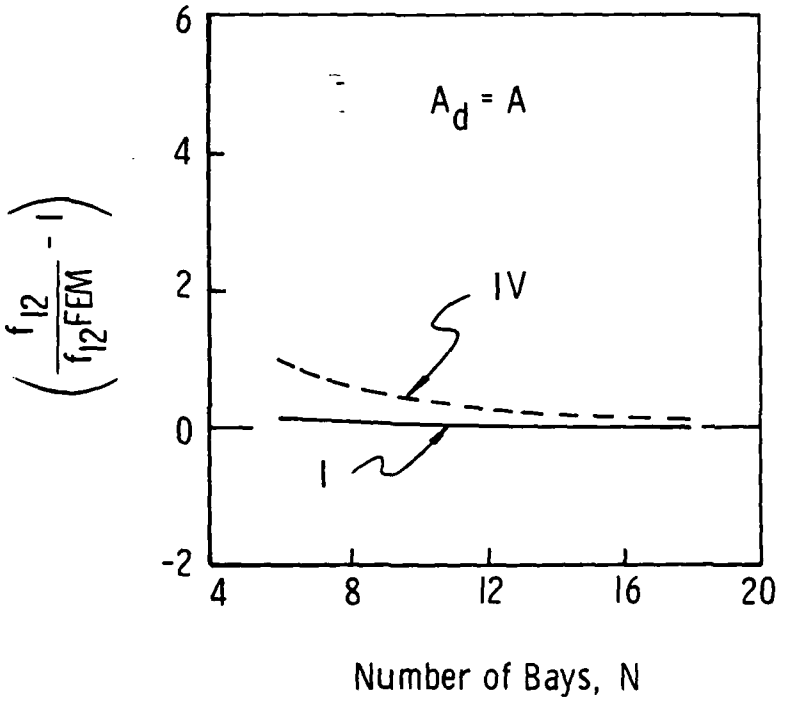

Fig. 10. Comparison of Natural Frequencies - Third Mode

Table 8. Comparison of Natural Frequencies - Fourth Mode

CASE A: $A_d = A$				
f_{22} \ N	6	8	12	18
FEM	31.80	23.64	12.86	6.76
I	35.40	24.16	13.25	6.75
II	35.80	24.51	13.44	6.82
III	61.10	36.41	16.94	7.69
IV	70.51	39.66	17.63	7.84

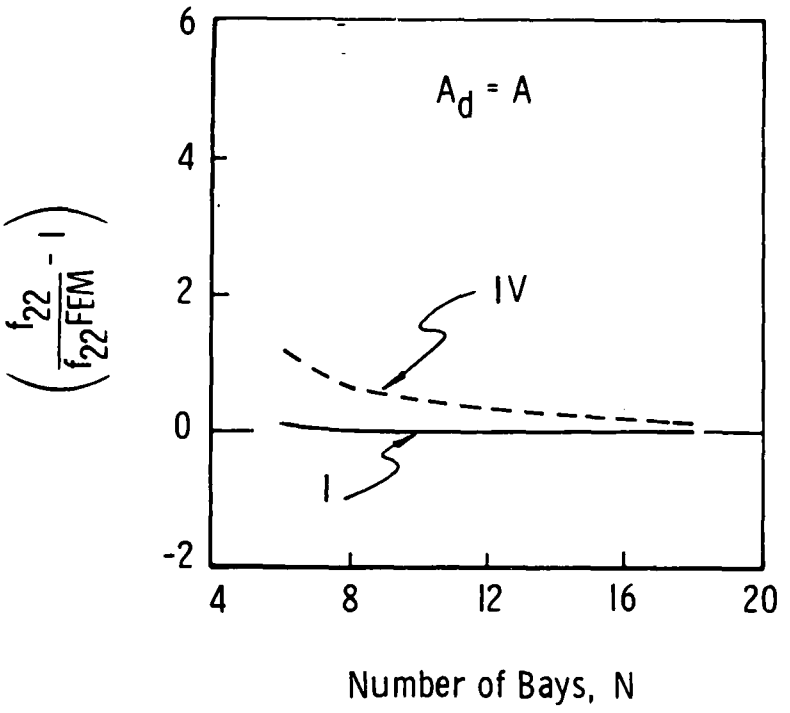

Fig. 11. Comparison of Natural Frequencies - Fourth Mode

Table 9. Comparison of Natural Frequencies - First Mode

CASE B: $A_d = 0.05A$				
f_{11} \ N	6	8	12	18
FEM	5.31	3.92	2.49	1.51
I	5.43	3.98	2.48	1.47
II	5.44	3.98	2.49	1.47
III	20.29	11.66	5.26	2.36
IV	21.39	11.99	5.33	2.37

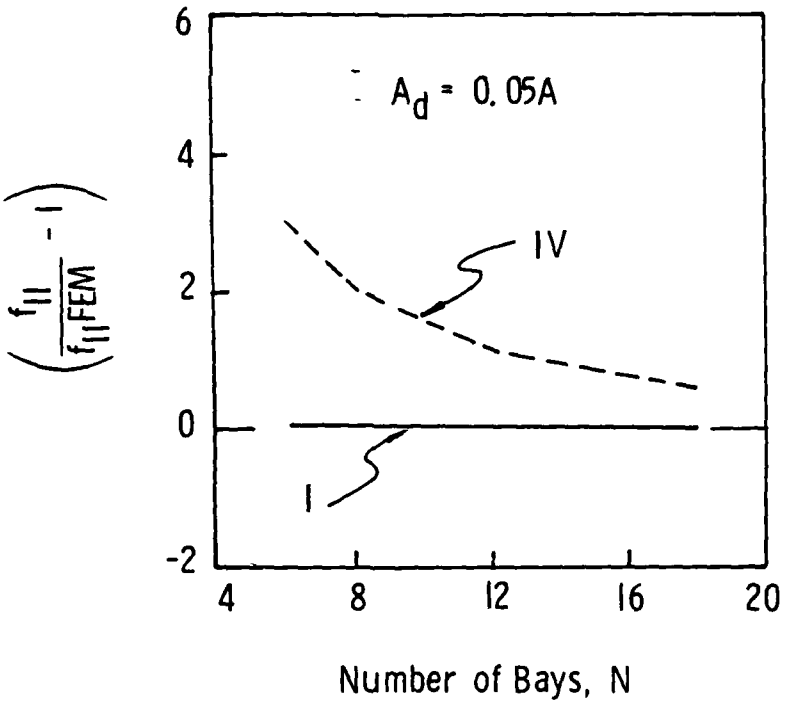

Fig. 12. Comparison of Natural Frequencies - First Mode

Table 10. Comparison of Natural Frequencies - Second Mode

CASE B: A_d = 0.05A				
f_{21} \ N	6	8	12	18
FEM	7.91	5.96	3.90	2.46
I	8.37	6.21	4.01	2.51
II	8.37	6.21	4.01	2.51
III	43.78	25.74	11.84	5.35
IV	48.74	27.42	12.19	5.42

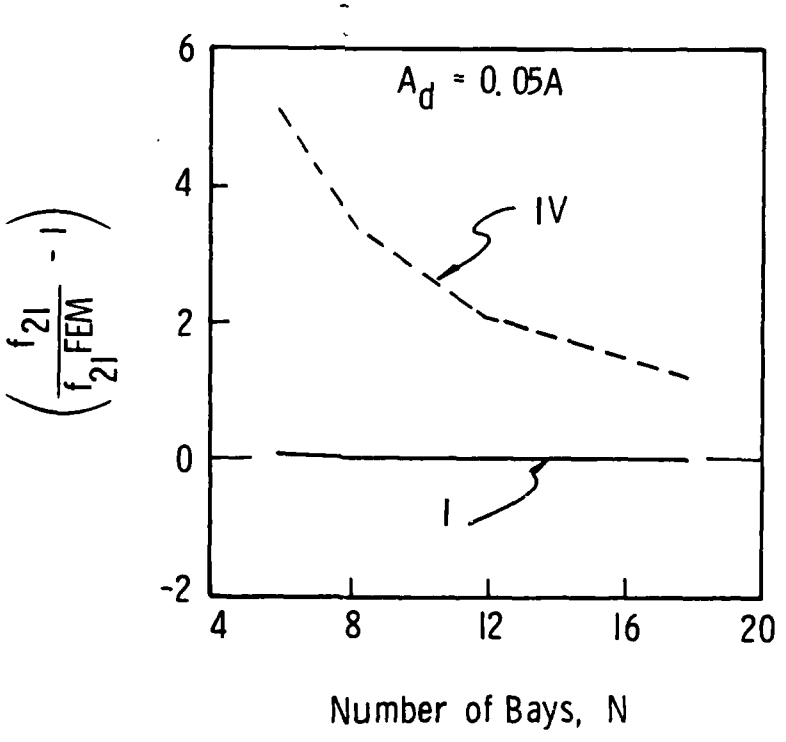

Fig. 13. Comparison of Natural Frequencies - Second Mode

Table 11. *Comparison of Natural Frequencies - Third Mode*

CASE B: $A_d = 0.05A$				
f_{12} \ N	6	8	12	18
FEM	8.92	6.68	4.36	2.75
I	9.14	6.79	4.41	2.78
II	9.14	6.79	4.41	2.78
III	51.07	30.23	13.98	6.33
IV	57.88	32.56	14.47	6.43

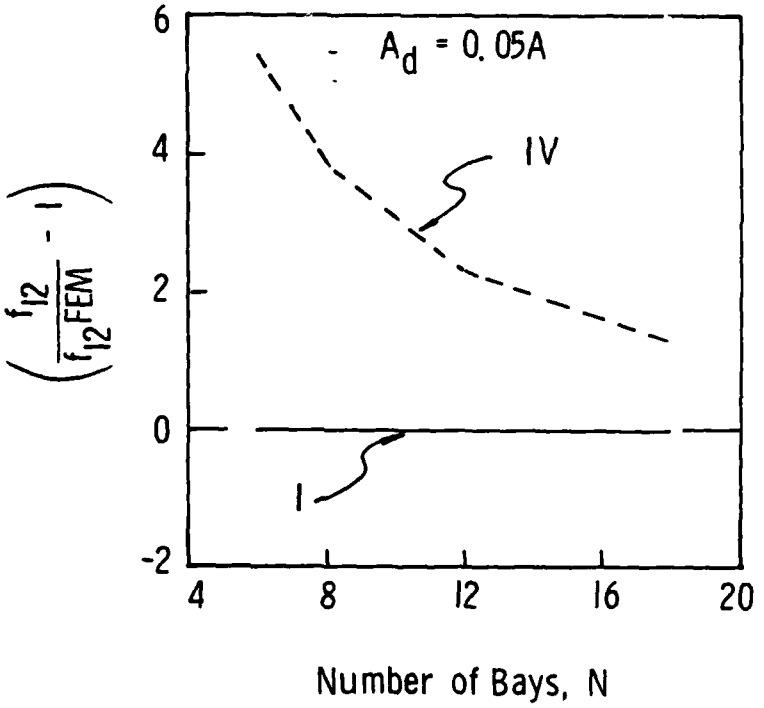

Fig. 14. Comparison of Natural Frequencies - Third Mode

Table 12. Comparison of Natural Frequencies - Fourth Mode

CASE B: A_d = 0.05A				
f_{22} \ N	6	8	12	18
FEM	10.63	8.04	5.33	3.43
I	11.15	8.30	5.43	3.48
II	11.15	8.30	5.43	3.48
III	71.60	43.16	20.29	9.26
IV	86.30	47.98	21.33	9.48

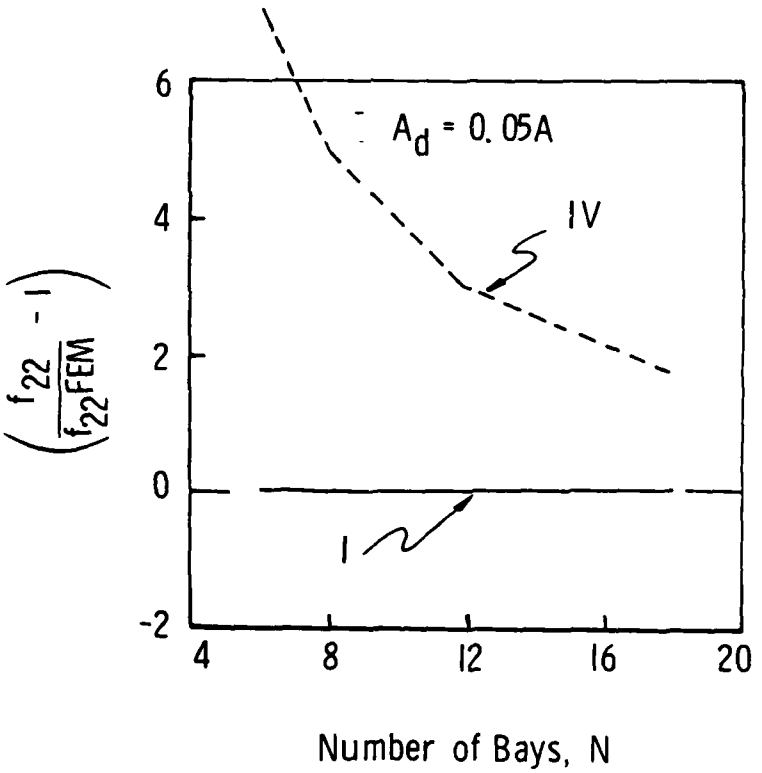

Fig. 15. Comparison of Natural Frequencies - Fourth Mode

Vibration Modes
12 x 12 Tetrahedral Truss Structural Model
Simply Supported Boundary Conditions

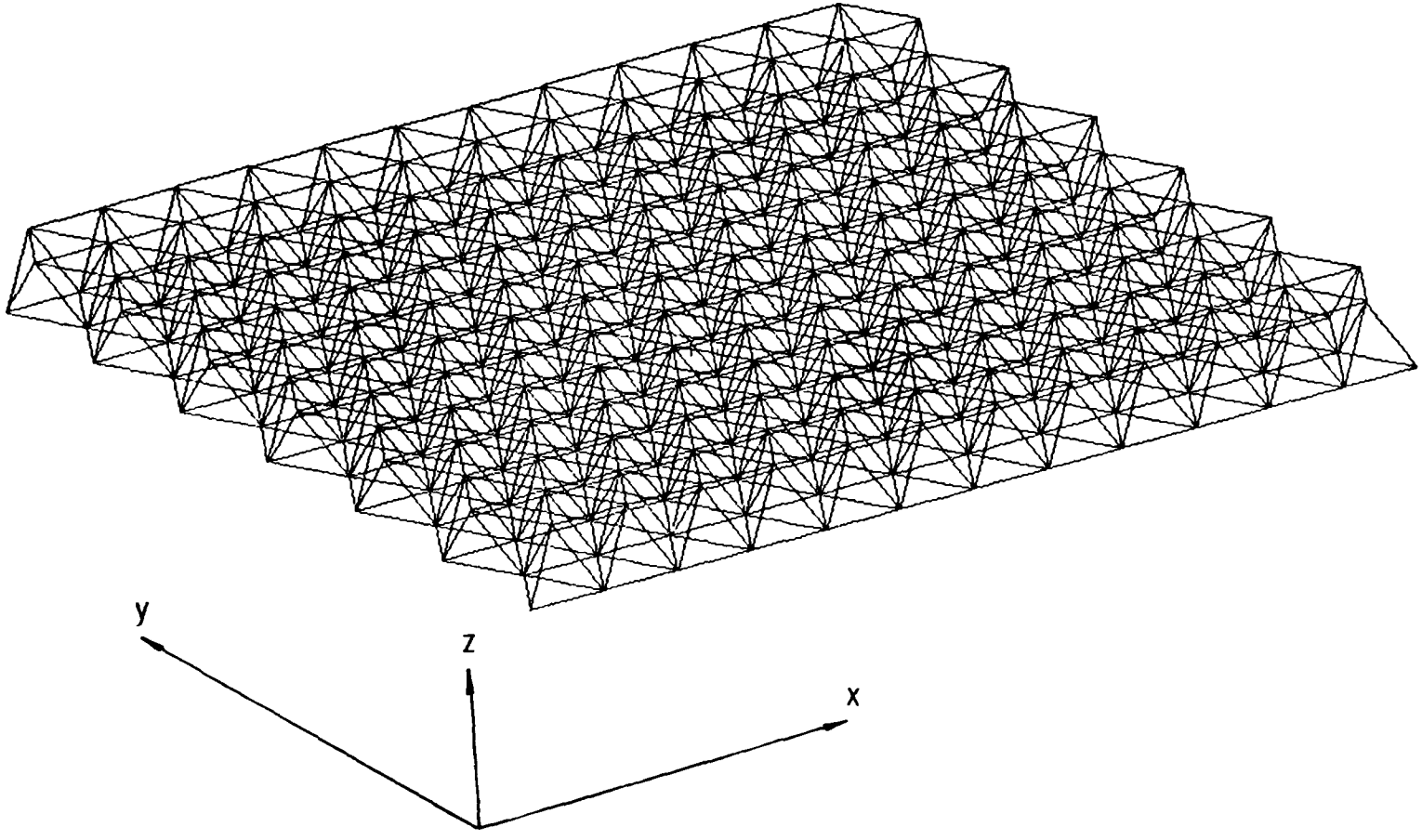

Fig. 16. Undeformed Shape - Orthographic View
(Simply Supported Boundary Conditions)

Vibration Modes
12 x 12 Tetrahedral Truss Structural Model
Simply Supported Boundary Conditions

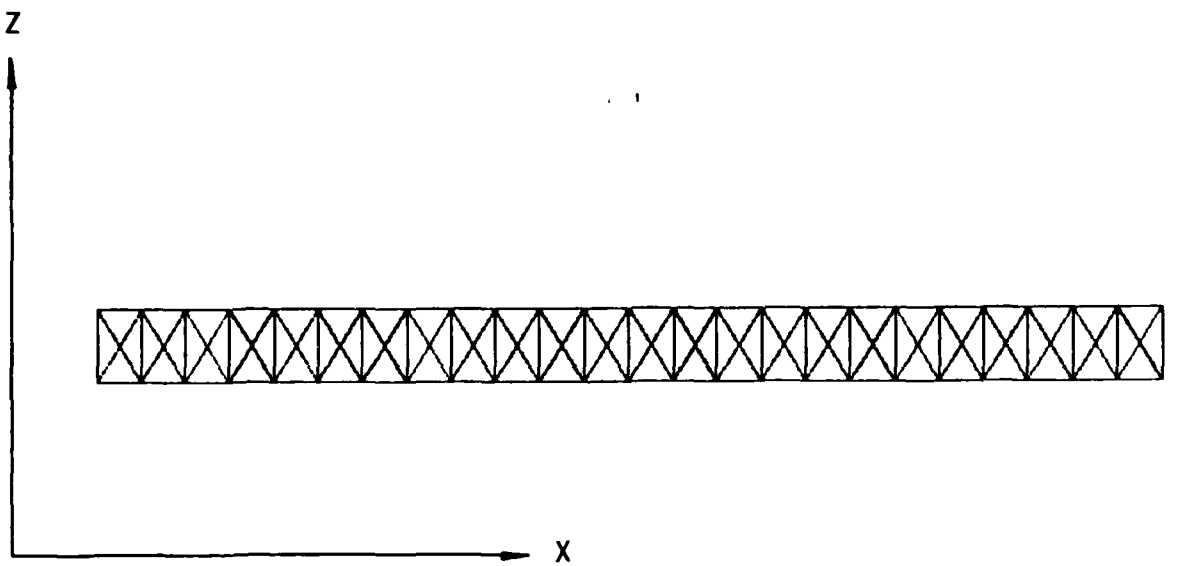

Fig. 17. Undeformed Shape - X-Z Plane Projection
(Simply Supported Boundary Conditions)

Vibration Modes
12 x 12 Tetrahedral Truss Structural Model
Simply Supported Boundary Conditions

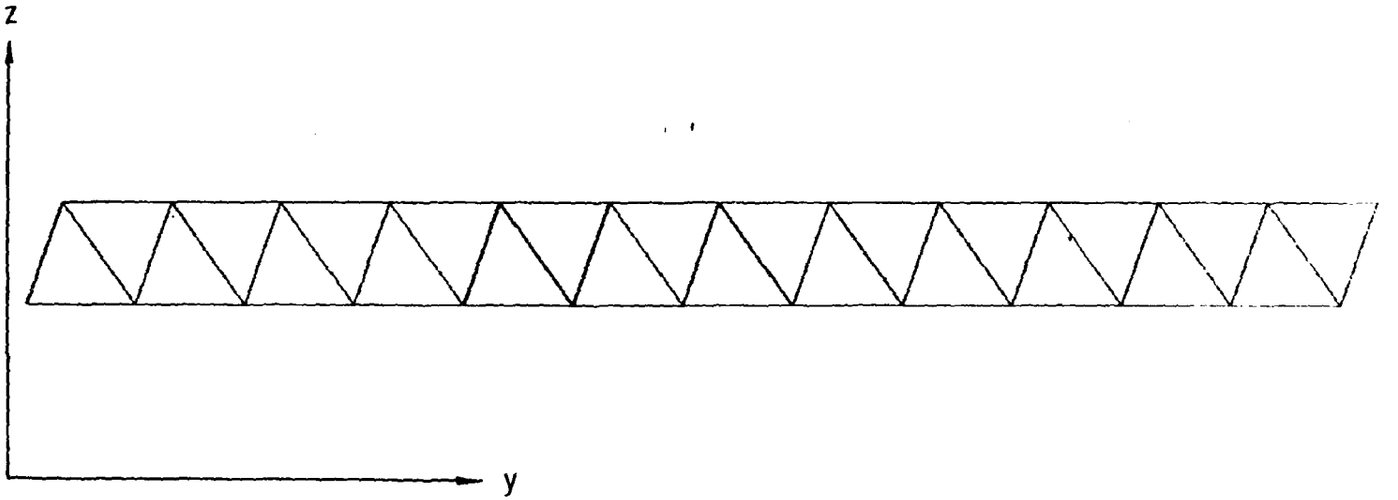

Fig. 18. Undeformed Shape - Y-Z Plane Projection
(Simply Supported Boundary Conditions)

Vibration Modes
12 x 12 Tetrahedral Truss Structural Model
Simply Supported Boundary Conditions

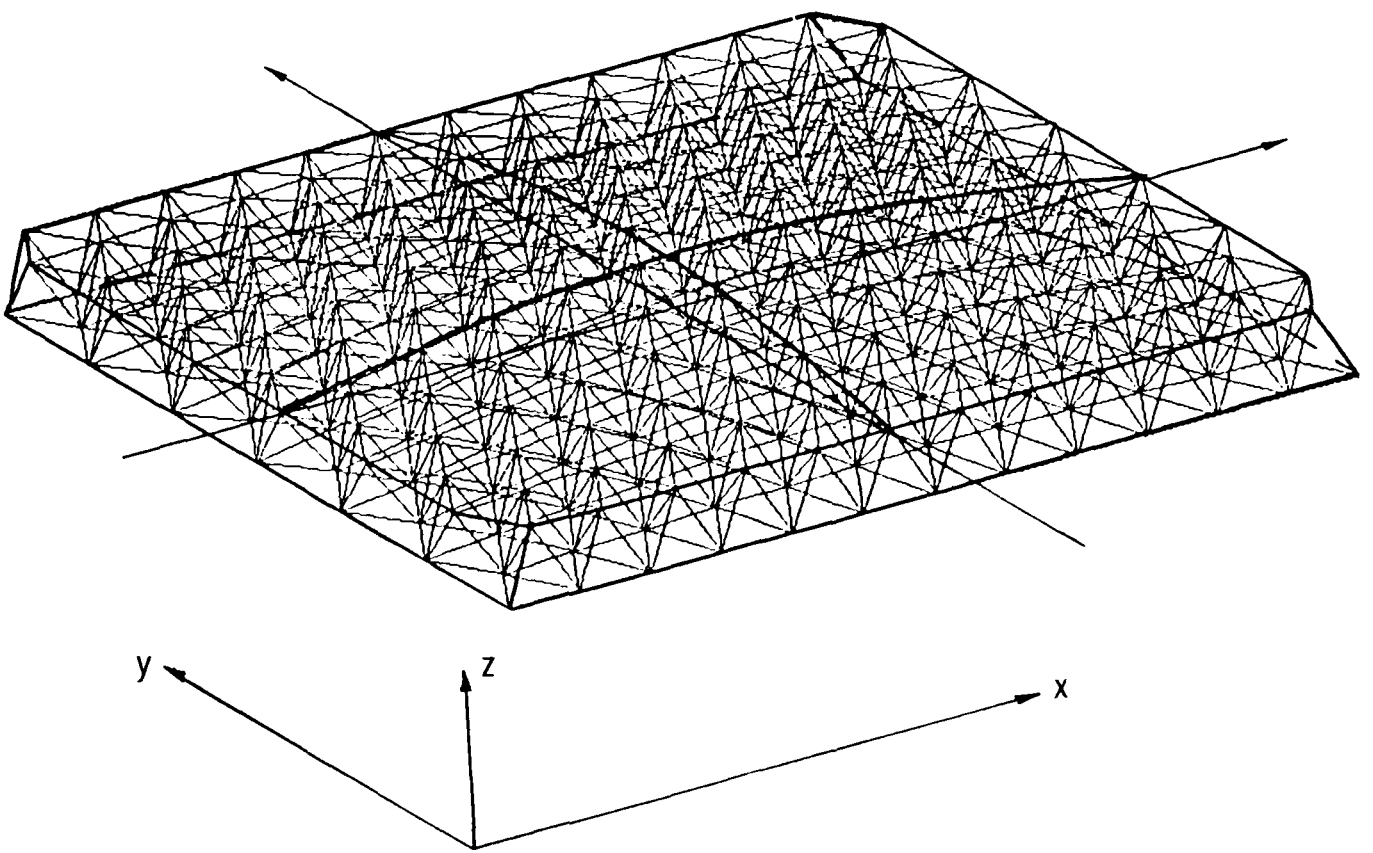

Fig. 19. First Mode - Orthographic View
(Simply Supported Boundary Conditions)

Vibration Modes
12 x 12 Tetrahedral Truss Structural Model
Simply Supported Boundary Conditions

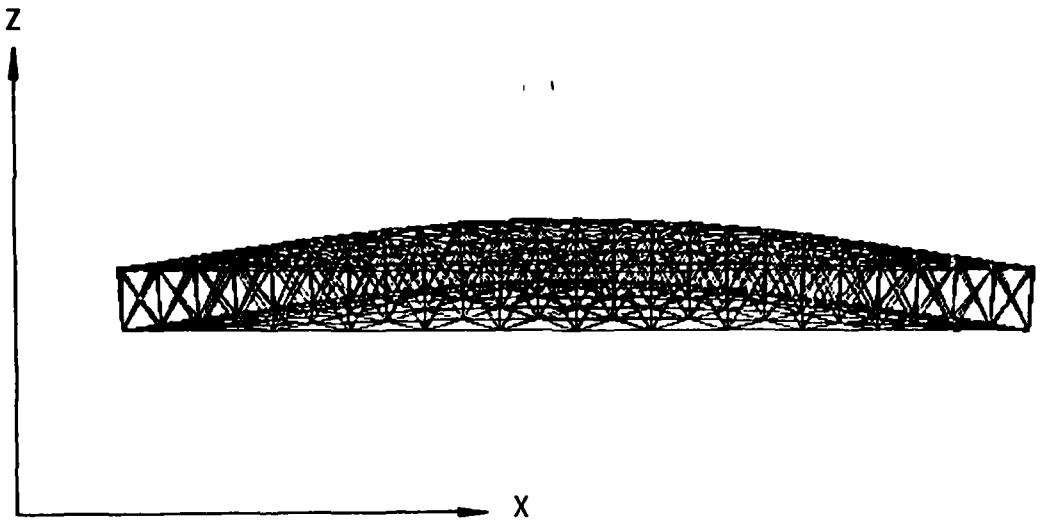

Fig. 20. First Mode - X-Z Plane Projection
(Simply Supported Boundary Conditions)

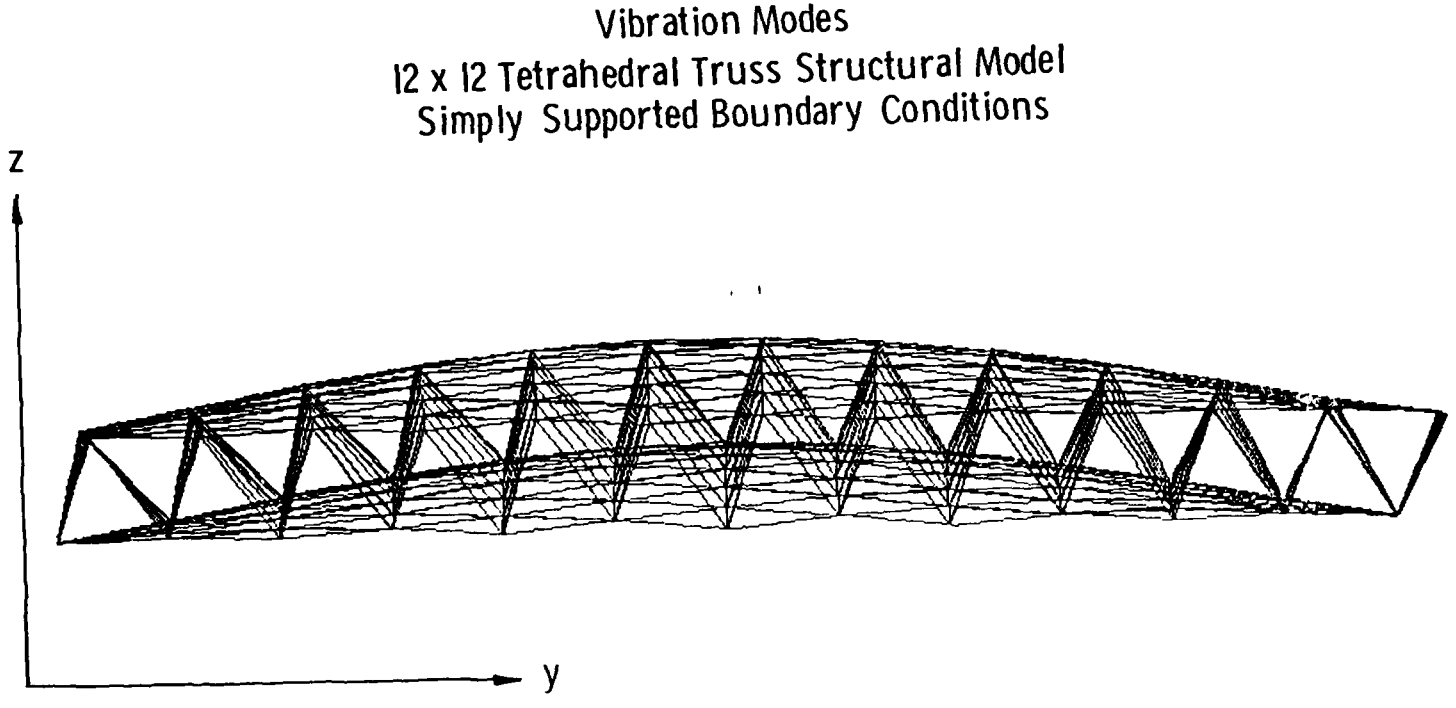

Fig. 21. First Mode - Y-Z Plane Projection
(Simply Supported Boundary Conditions)

Vibration Modes
12 x 12 Tetrahedral Truss Structural Model
Simply Supported Boundary Conditions

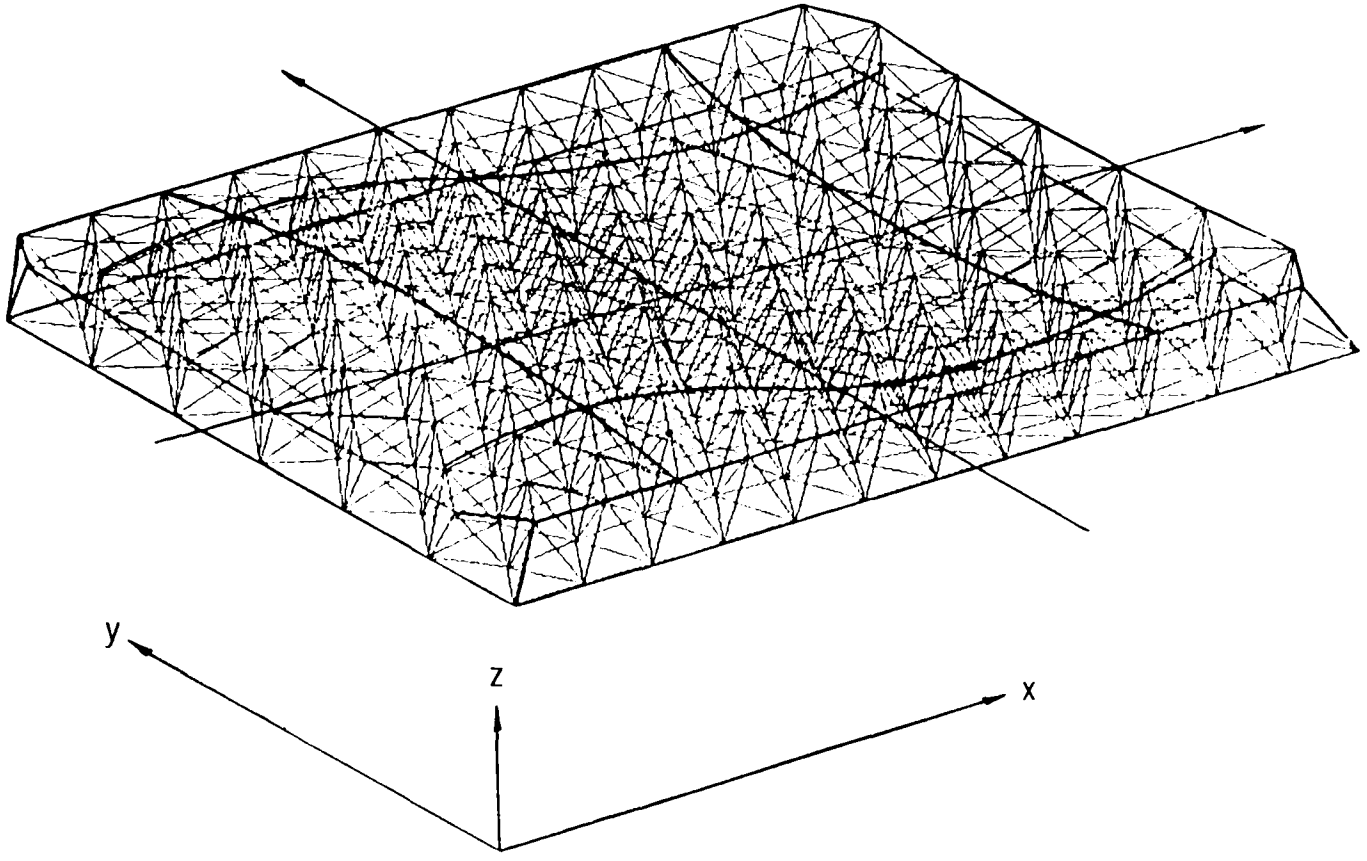

Fig. 22. Second Mode - Orthographic View
(Simply Supported Boundary Conditions)

Vibration Modes
12 x 12 Tetrahedral Truss Structural Model
Simply Supported Boundary Conditions

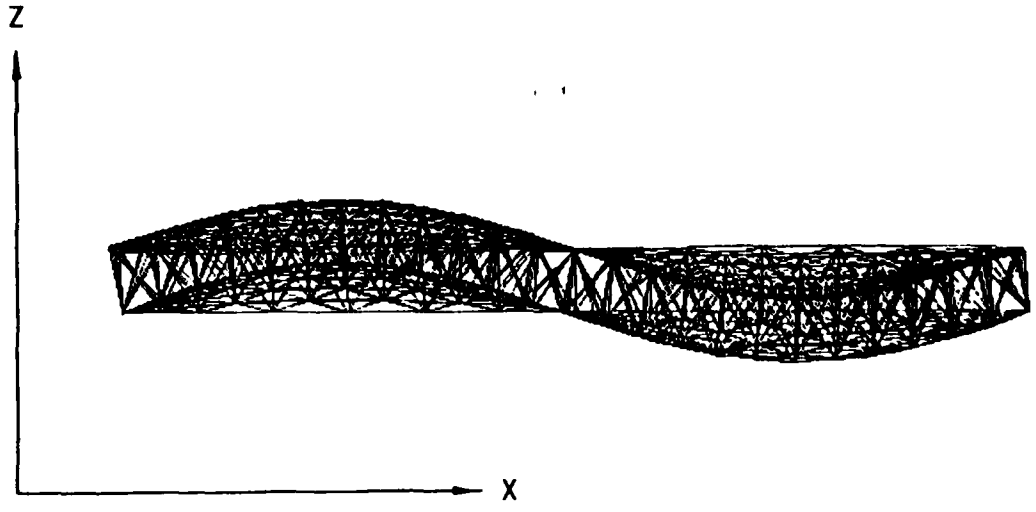

Fig. 23. Second Mode - X-Z Plane Projection
(Simply Supported Boundary Conditions)

Vibration Modes
12 x 12 Tetrahedral Truss Structural Model
Simply Supported Boundary Conditions

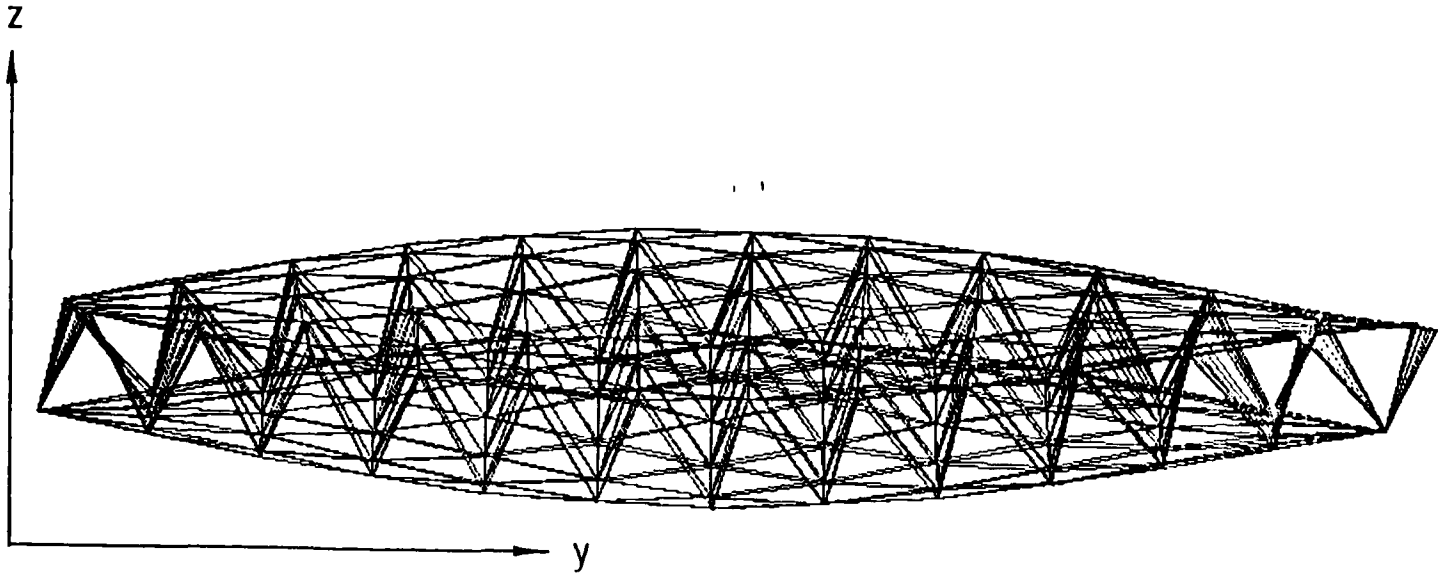

Fig. 24. Second Mode - Y-Z Plane Projection
(Simply Supported Boundary Conditions)

Vibration Modes
12 x 12 Tetrahedral Truss Structural Model
Simply Supported Boundary Conditions

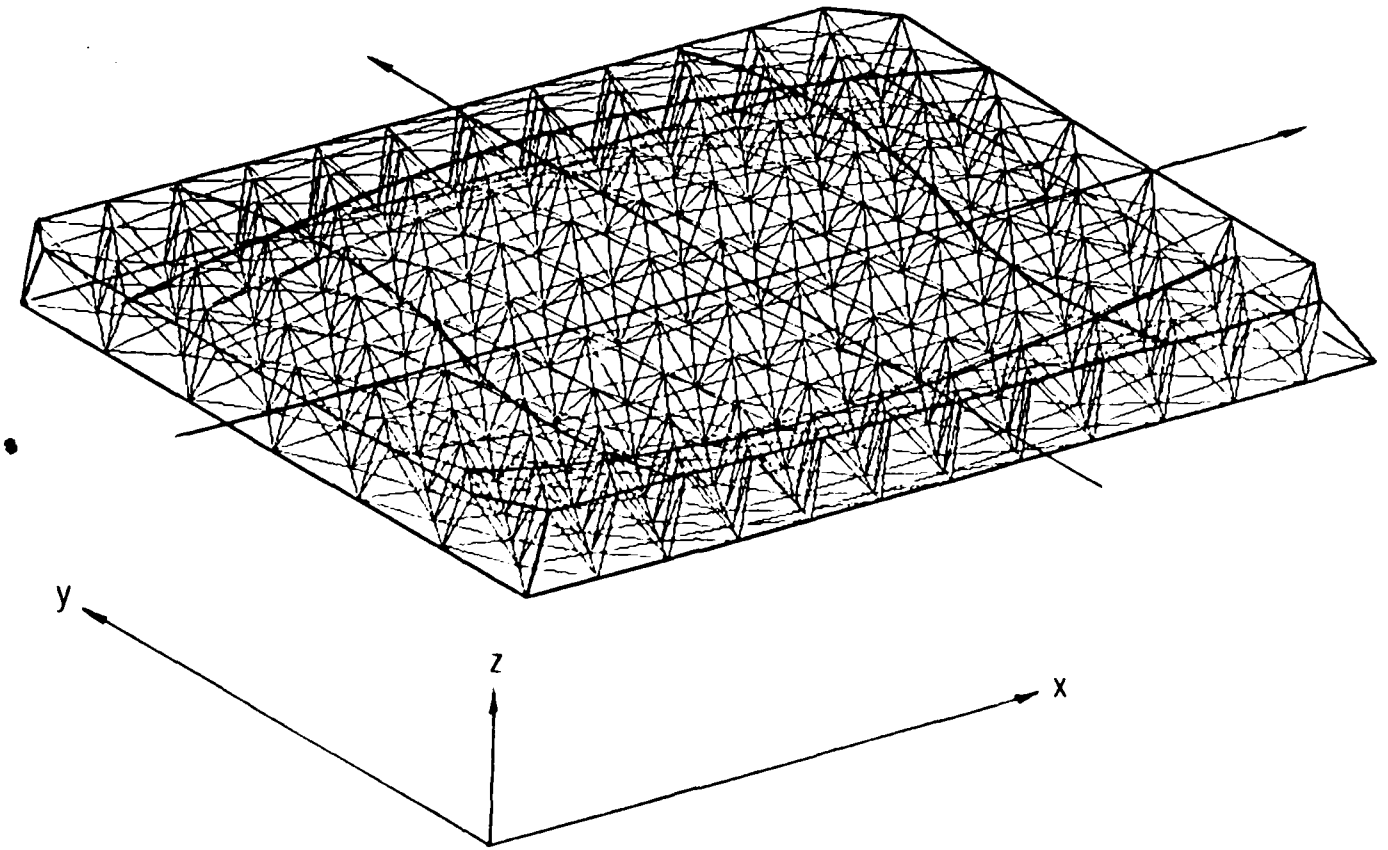

Fig. 25. Third Mode - Orthographic View
(Simply Supported Boundary Conditions)

Vibration Modes
12 x 12 Tetrahedral Truss Structural Model
Simply Supported Boundary Conditions

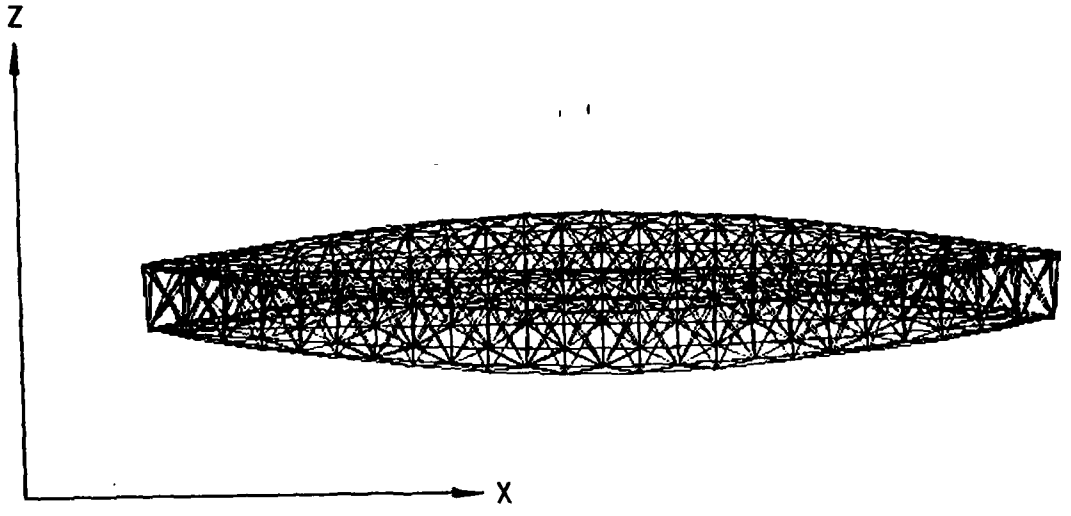

Fig. 26. Third Mode - X-Z Plane Projection
(Simply Supported Boundary Conditions)

Vibration Modes
12 x 12 Tetrahedral Truss Structural Model
Simply Supported Boundary Conditions

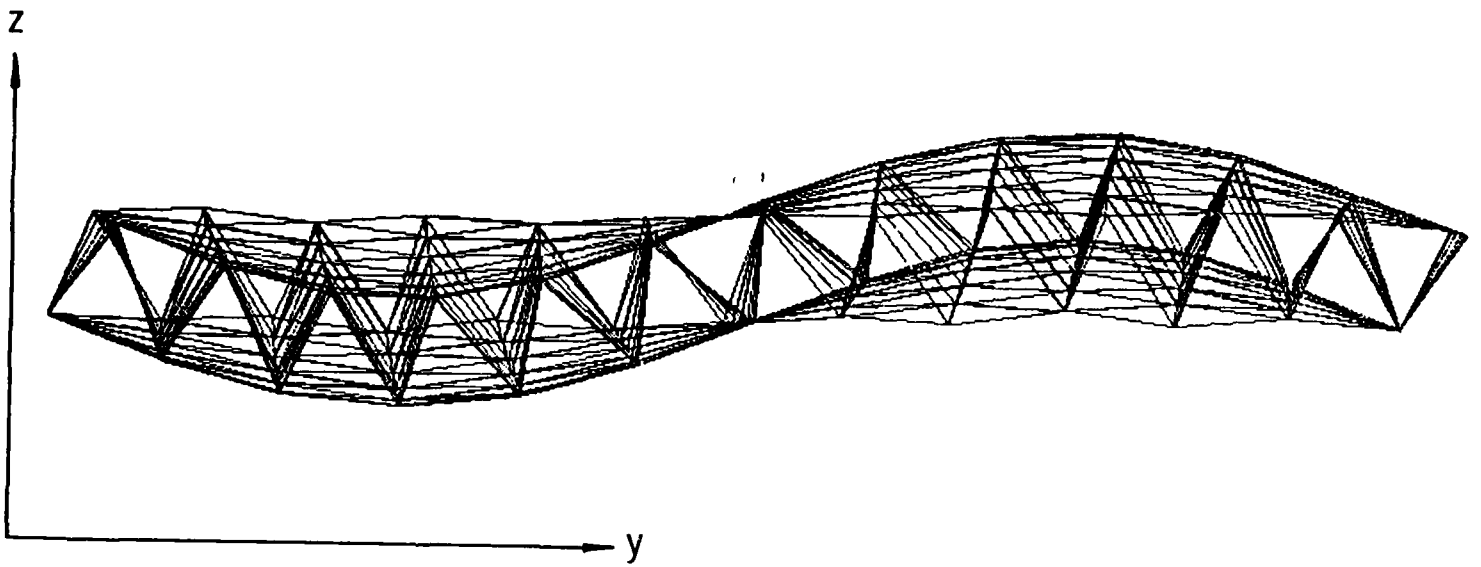

Fig. 27. Third Mode - Y-Z Plane Projection
(Simply Supported Boundary Conditions)

Vibration Modes
12 x 12 Tetrahedral Truss Structural Model
Simply Supported Boundary Conditions

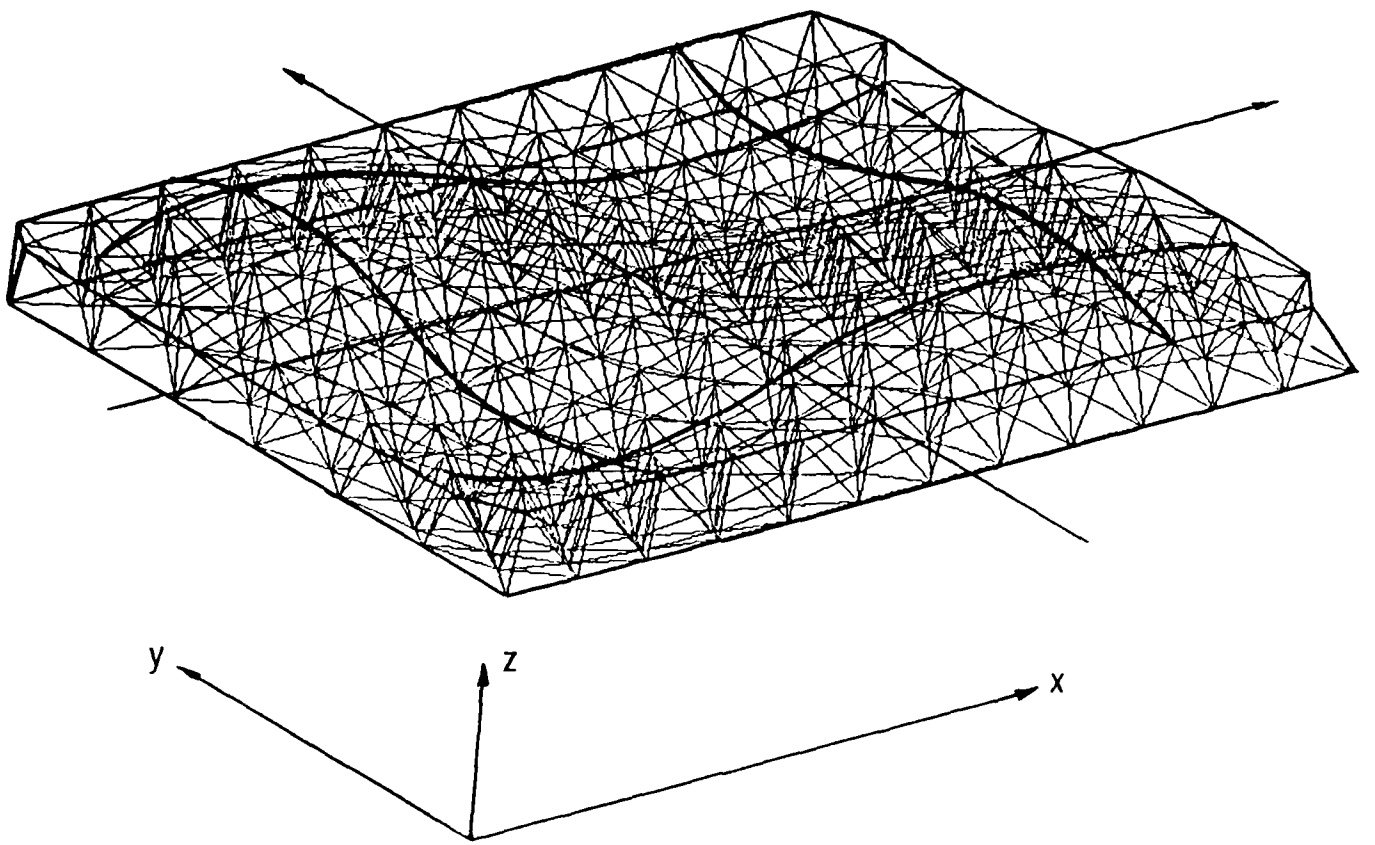

Fig. 28. Fourth Mode - Orthographic View
(Simply Supported Boundary Conditions)

Vibration Modes
12 x 12 Tetrahedral Truss Structural Model
Simply Supported Boundary Conditions

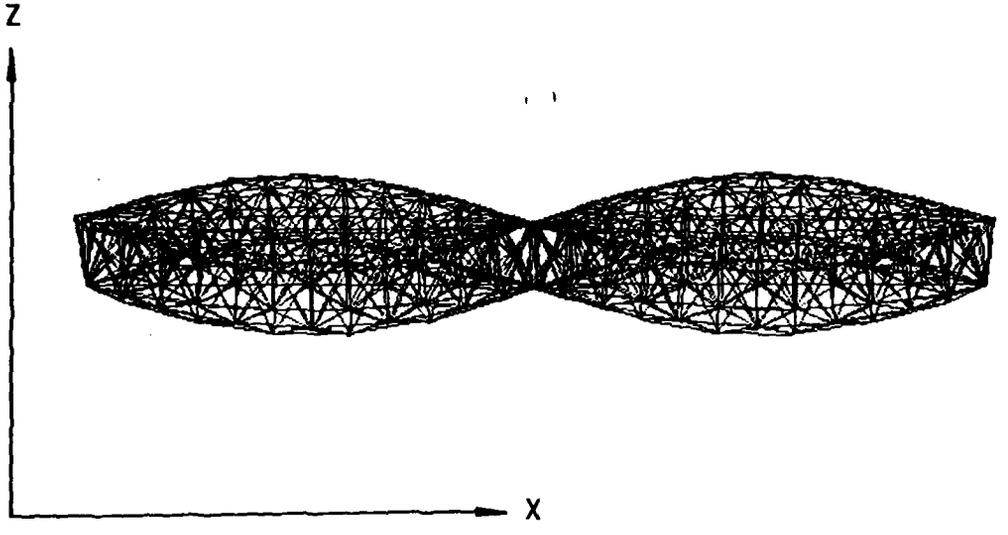

Fig. 29. Fourth Mode - X-Z Plane Projection
(Simply Supported Boundary Conditions)

Vibration Modes
12 x 12 Tetrahedral Truss Structural Model
Simply Supported Boundary Conditions

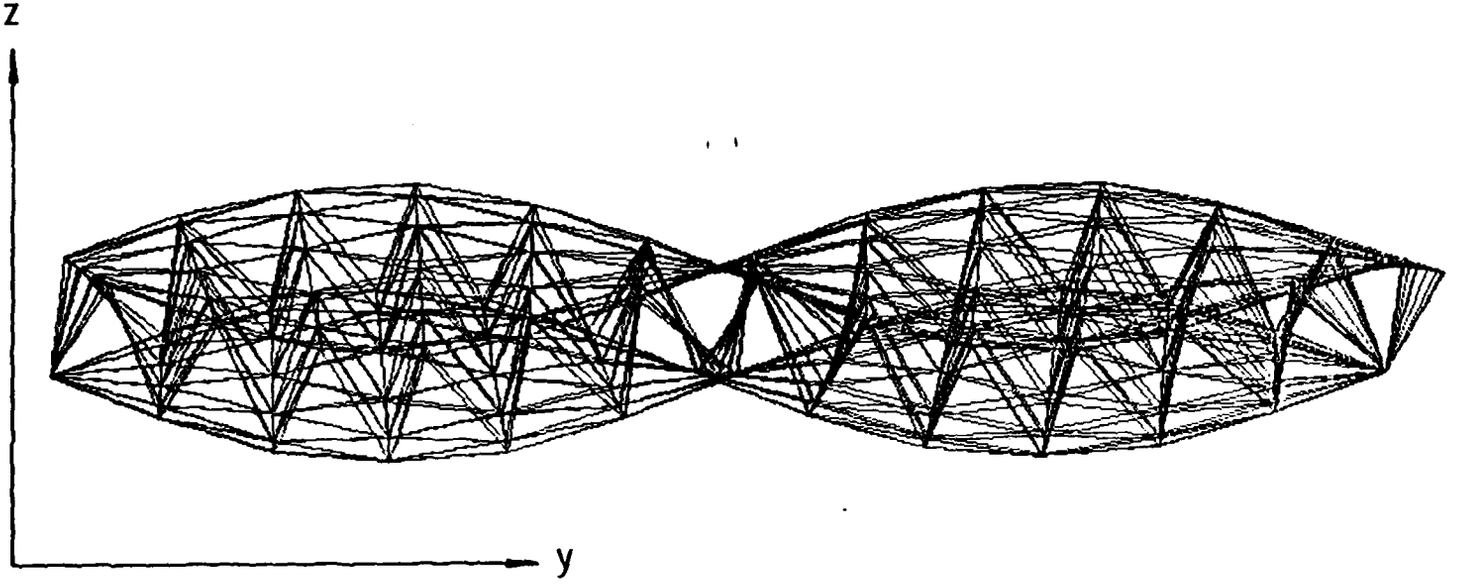

Fig. 30. Fourth Mode - Y-Z Plane Projection
(Simply Supported Boundary Conditions)

Numerical results, presented for the simply supported tetrahedral truss, demonstrate the accuracy obtainable from the equivalent continuum model. It is observed that, in most instances, the error is less than 3 percent. Furthermore, the four solutions, I through IV, demonstrate the significance of including the transverse shear and rotary inertia terms in formulating the equivalent plate problem. It is observed that Solution I, which includes both the transverse shear and rotary inertia effects, is very good even when the number of basic repeating truss elements is small. The effect of transverse shear, which is quite significant for a truss with a small number of repeating elements, becomes less pronounced as the number of these elements increases. This is shown in Figs. 8 through 15. The rotary inertia effect, on the other hand, is important only for higher frequency responses and for a smaller number of repeating elements. Yet, its effect is much less pronounced than that of the transverse shear (see Tables 5 through 12). Furthermore, it is also observed that the effect of transverse shear is much more significant for the case in which $A_d = 0.05A$. Finally, the mode shapes shown in Figs. 16 through 30 exhibit striking similarities to those of a plate with simply supported boundary conditions.

In the second example case, free-free boundary conditions are assumed. The natural frequencies for the truss are determined, as in the first case, using the NASTRAN computer program. Since, for the free-free boundary condition, the closed form solution is not readily available for the equivalent continuum plate, the natural frequencies are determined using the NASTRAN computer program. A procedure given by MacNeal (Ref. 33) is followed for this purpose.

---

[33]MacNeal, R. H., "A Simple Quadrilateral Shell Element," Computer and Structures, Vol. 8, 1978.

It may be noted here that the finite element solution of a free-free plate accounts for transverse shear only. The natural frequencies computed for the truss as well as for the equivalent continuum model are given in Tables 13 and 14.

Table 13. Comparison of Natural Frequencies, Free-Free Boundary Conditions

CASE A: $A_d = A$				
Frequency \ N		6	12	18
First Mode f_{11}	Truss	8.63	2.56	1.20
	Continuum Model	9.29	2.66	1.23
Second Mode f_{21}	Truss	12.47	3.72	1.72
	Continuum Model	13.81	3.87	1.76
Third Mode f_{12}	Truss	15.43	4.91	2.34
	Continuum Model	18.56	5.50	2.56
Fourth Mode f_{22}	Truss	18.80	6.11	2.92
	Continuum Model	20.07	6.35	3.02

Table 14. Comparison of Natural Frequencies, Free-Free Boundary Conditions

CASE B: A_d = 0.05A				
Frequency \ N		6	12	18
First Mode f_{11}	Truss	5.31	2.11	1.12
	Continuum Model	4.72	1.98	1.09
Second Mode f_{21}	Truss	7.22	3.02	1.64
	Continuum Model	6.61	2.87	1.60
Third Mode f_{12}	Truss	7.62	3.49	2.03
	Continuum Model	7.74	3.50	2.04
Fourth Mode f_{22}	Truss	8.74	3.88	2.26
	Continuum Model	7.76	3.59	2.15

The associated mode shapes (orthographic view, projections on the X-Z and Y-Z planes) are shown in Figs. 31 through 42. A good comparison is once again obtained between the truss model and its equivalent continuum model. The mode shapes (Figs. 31 through 42) are also similar to those of a free-free plate.

Vibration Modes
12 x 12 Tetrahedral Truss Structural Model
Free-Free Boundary Conditions

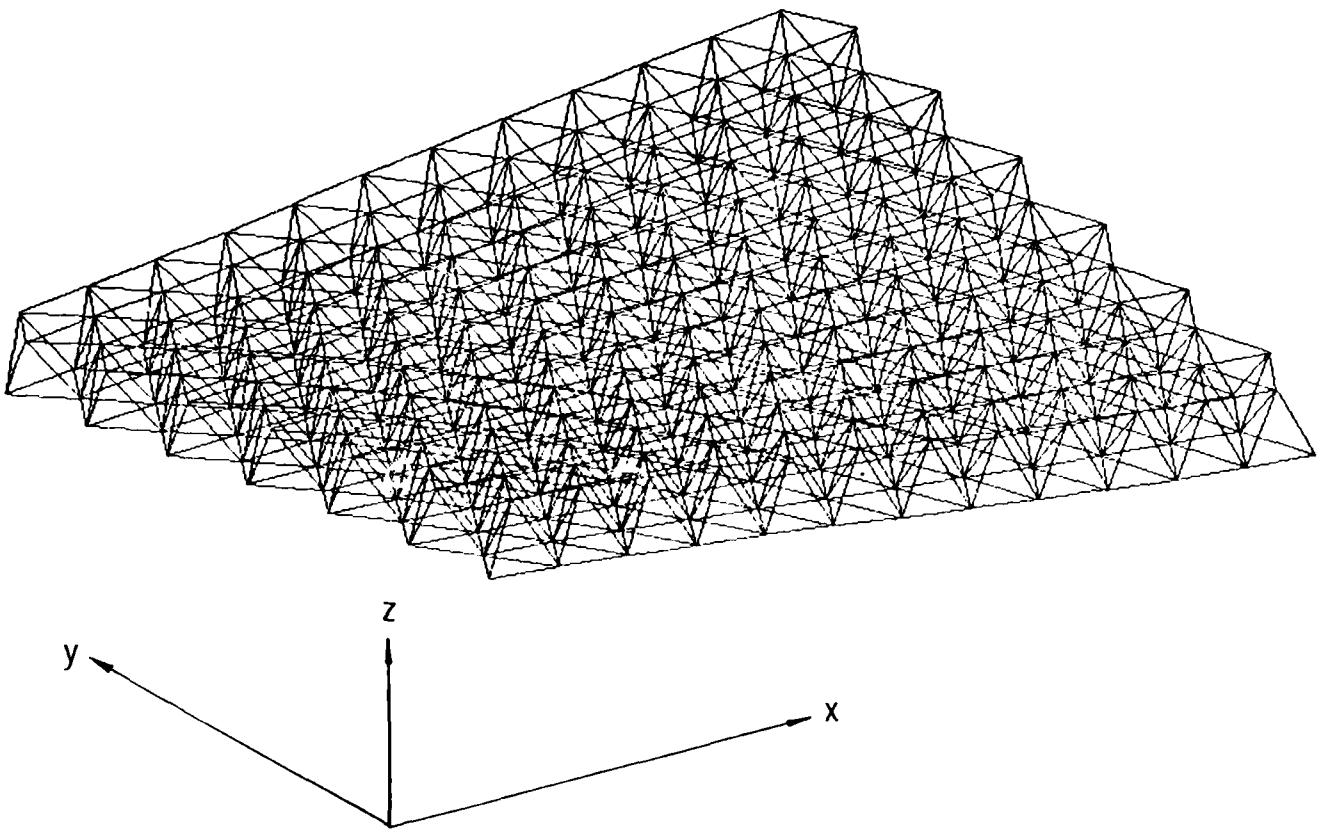

Fig. 31. First Mode - Orthographic View
(Free-Free Boundary Conditions)

Vibration Modes
12 x 12 Tetrahedral Truss Structural Model
Free-Free Boundary Conditions

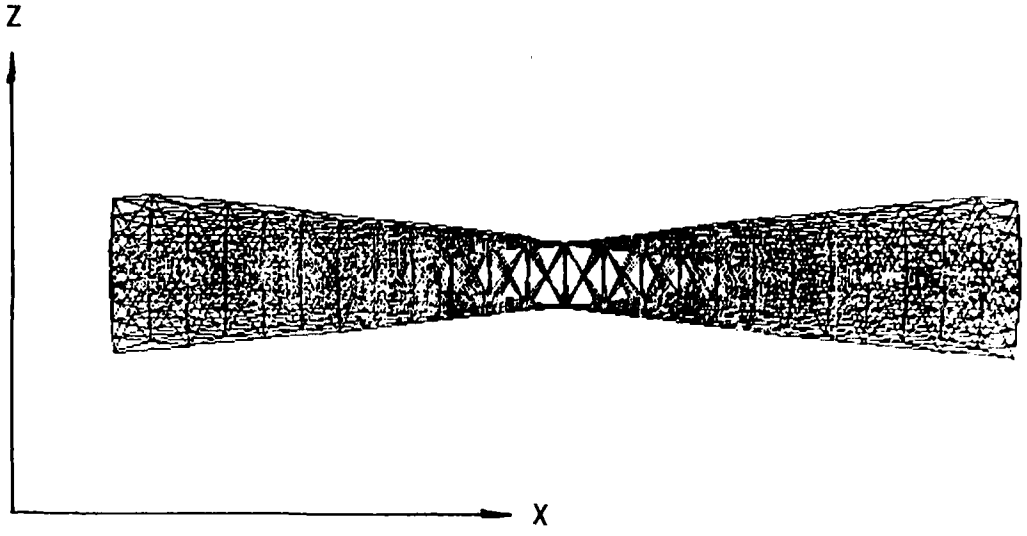

Fig. 32. First Mode - X-Z Plane Projection
(Free-Free Boundary Conditions)

Vibration Modes
12 x 12 Tetrahedral Truss Structural Model
Free-Free Boundary Conditions

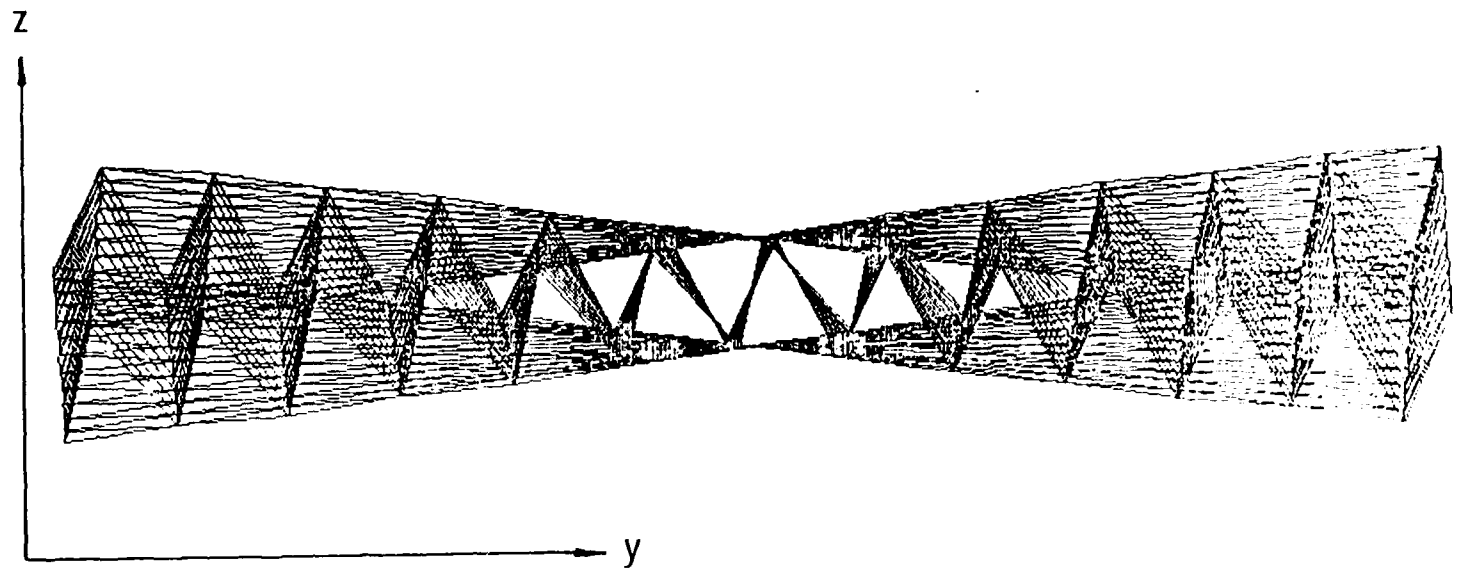

Fig. 33. First Mode - Y-Z Plane Projection
(Free-Free Boundary Conditions)

Vibration Modes
12 x 12 Tetrahedral Truss Structural Model
Free-Free Boundary Conditions

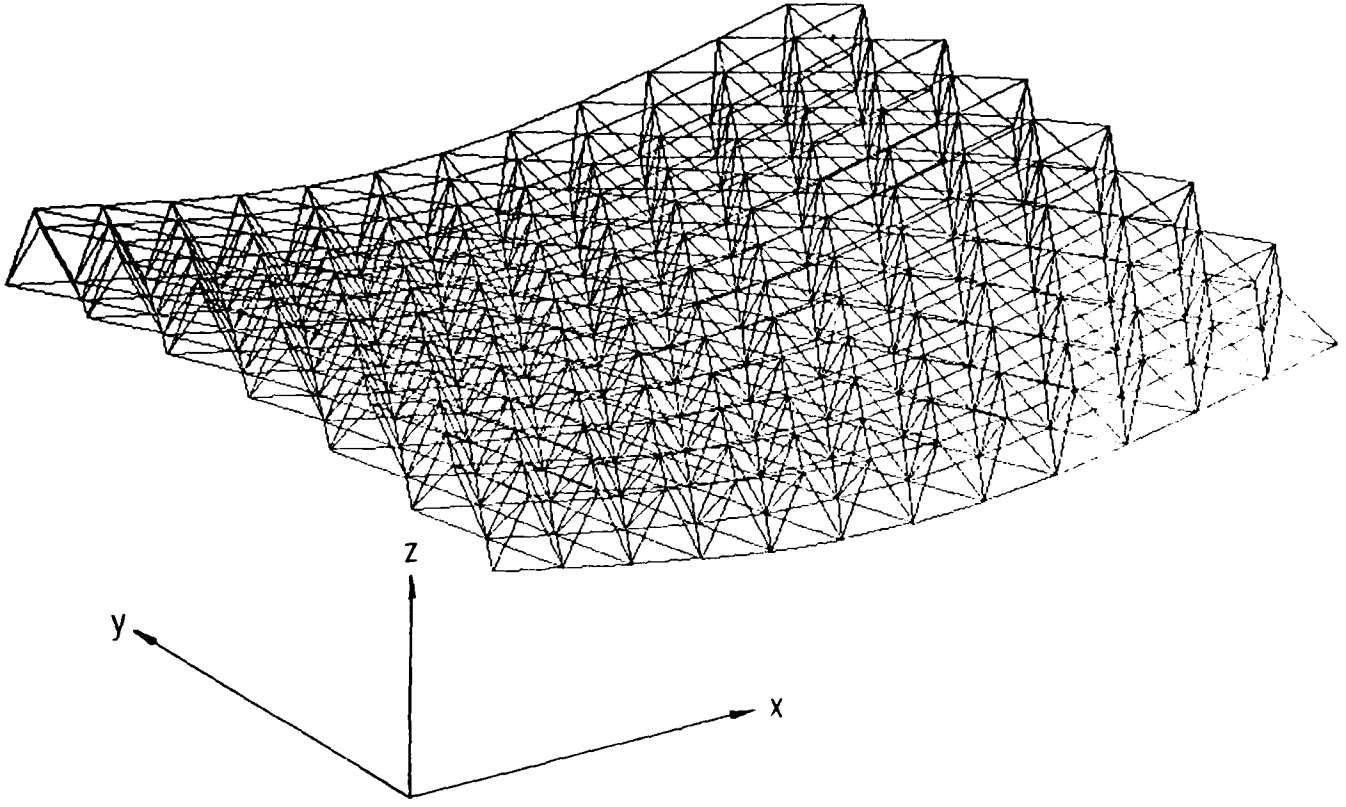

Fig. 34. Second Mode - Orthographic View
(Free-Free Boundary Conditions)

Vibration Modes
12 x 12 Tetrahedral Truss Structural Model
Free-Free Boundary Conditions

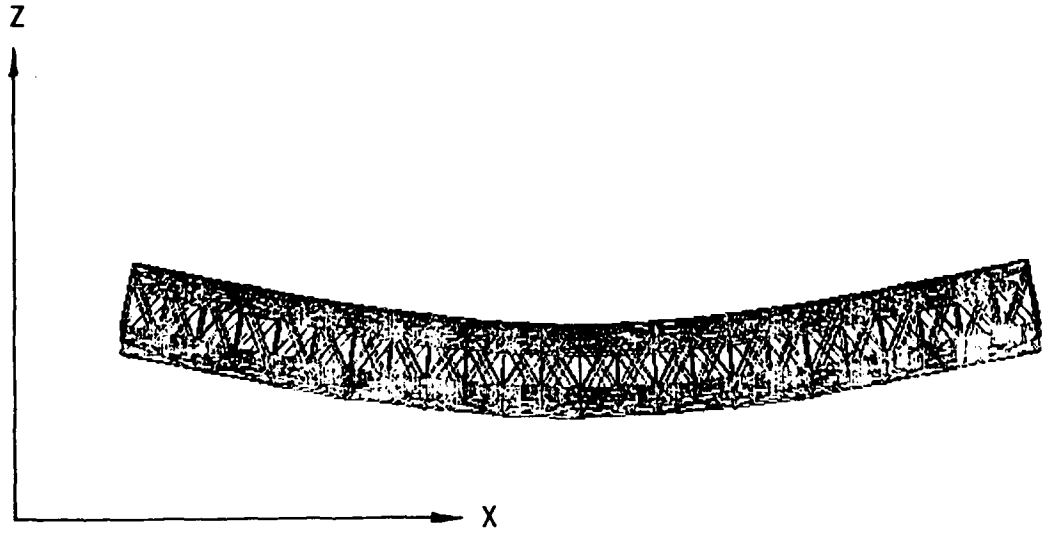

Fig. 35. Second Mode - X-Z Plane Projection
(Free-Free Boundary Conditions)

Vibration Modes
12 x 12 Tetrahedral Truss Structural Model
Free-Free Boundary Conditions

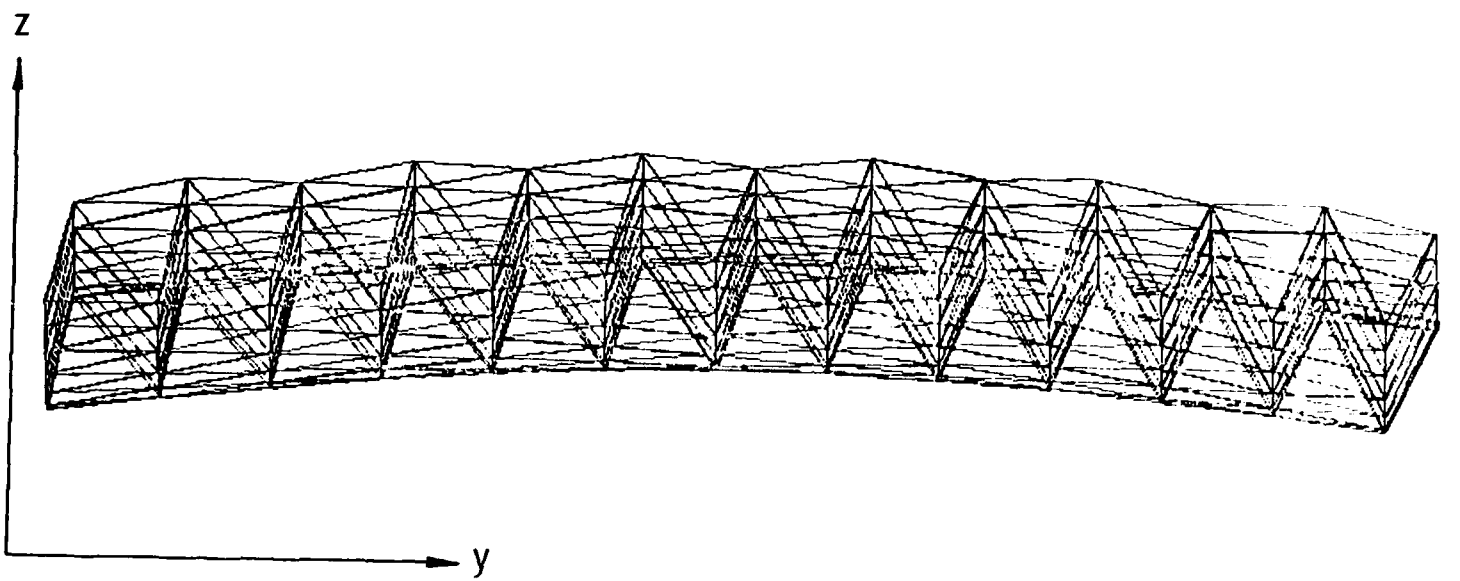

Fig. 36. Second Mode - Y-Z Plane Projection
(Free-Free Boundary Conditions

Vibration Modes
12 x 12 Tetrahedral Truss Structural Model
Free-Free Boundary Conditions

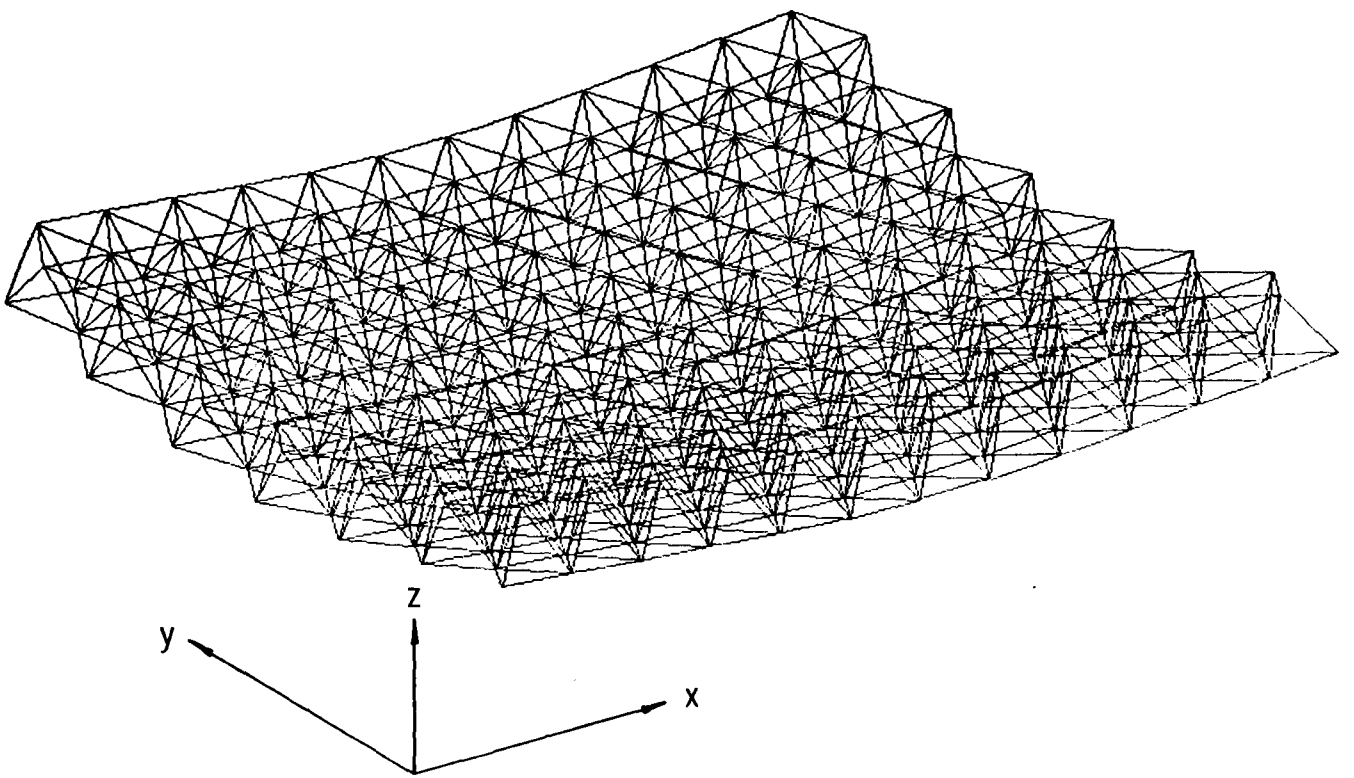

Fig. 37. Third Mode - Orthographic View
(Free-Free Boundary Conditions)

Vibration Modes
12 x 12 Tetrahedral Truss Structural Model
Free-Free Boundary Conditions

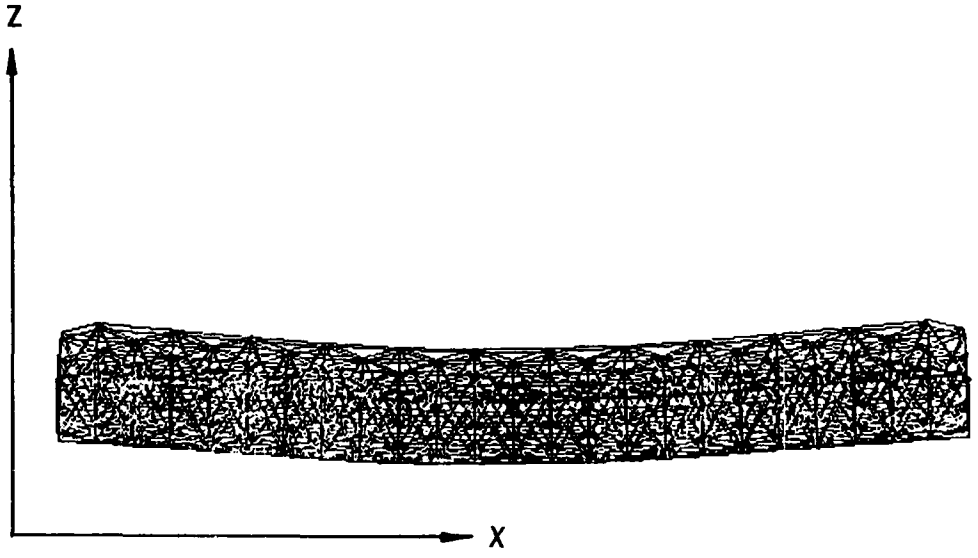

Fig. 38. Third Mode - X-Z Plane Projection
(Free-Free Boundary Conditions)

Vibration Modes
12 x 12 Tetrahedral Truss Structural Model
Free-Free Boundary Conditions

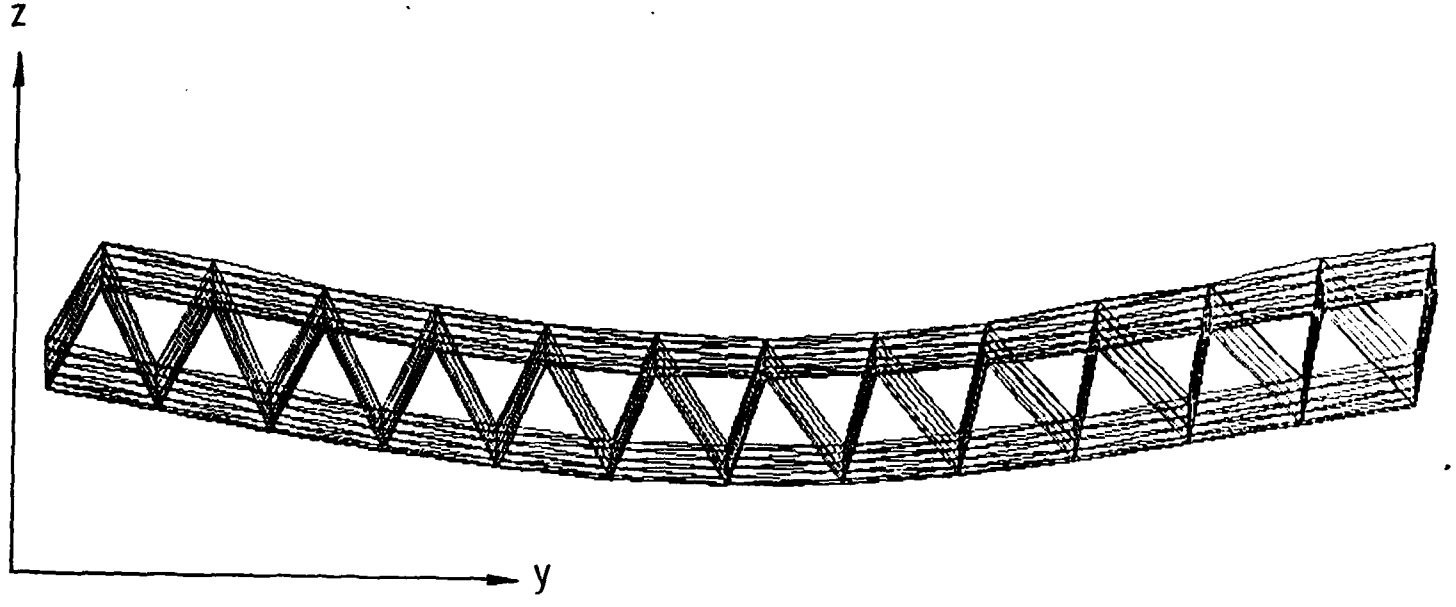

Fig. 39. Third Mode - Y-Z Plane Projection
(Free-Free Boundary Conditions)

Vibration Modes
12 x 12 Tetrahedral Truss Structural Model
Free-Free Boundary Conditions

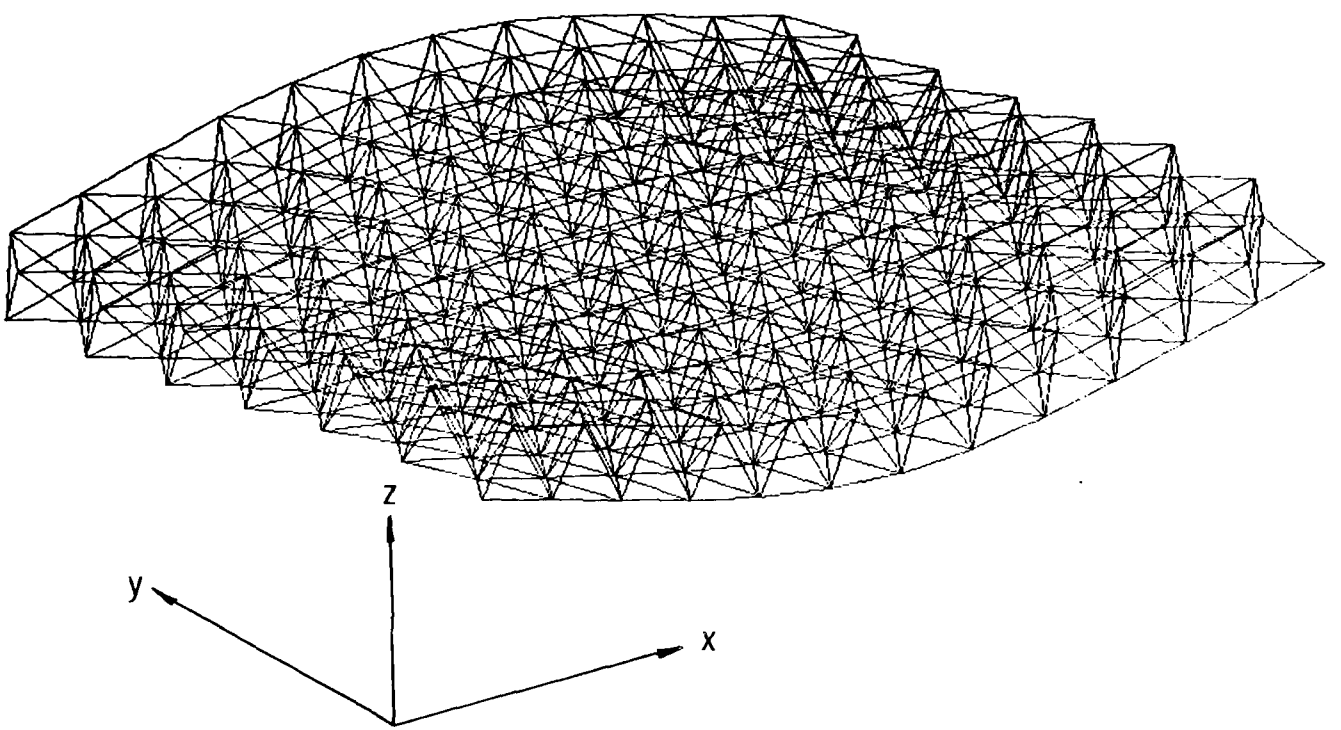

Fig. 40. Fourth Mode - Orthographic View
(Free-Free Boundary Conditions)

Vibration Modes
12 x 12 Tetrahedral Truss Structural Model
Free-Free Boundary Conditions

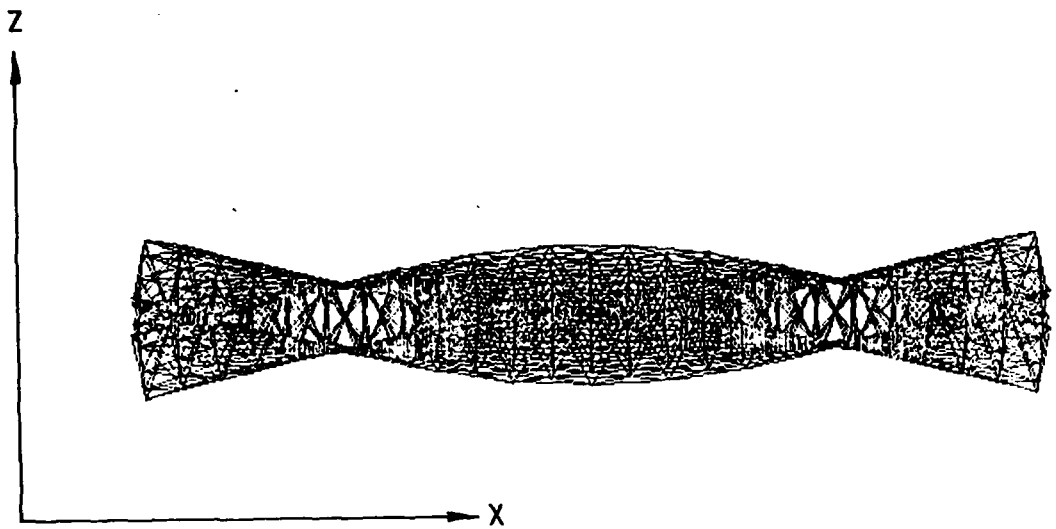

Fig. 41. Fourth Mode - X-Z Plane Projection
(Free-Free Boundary Conditions

Vibration Modes
12 x 12 Tetrahedral Truss Structural Model
Free-Free Boundary Conditions

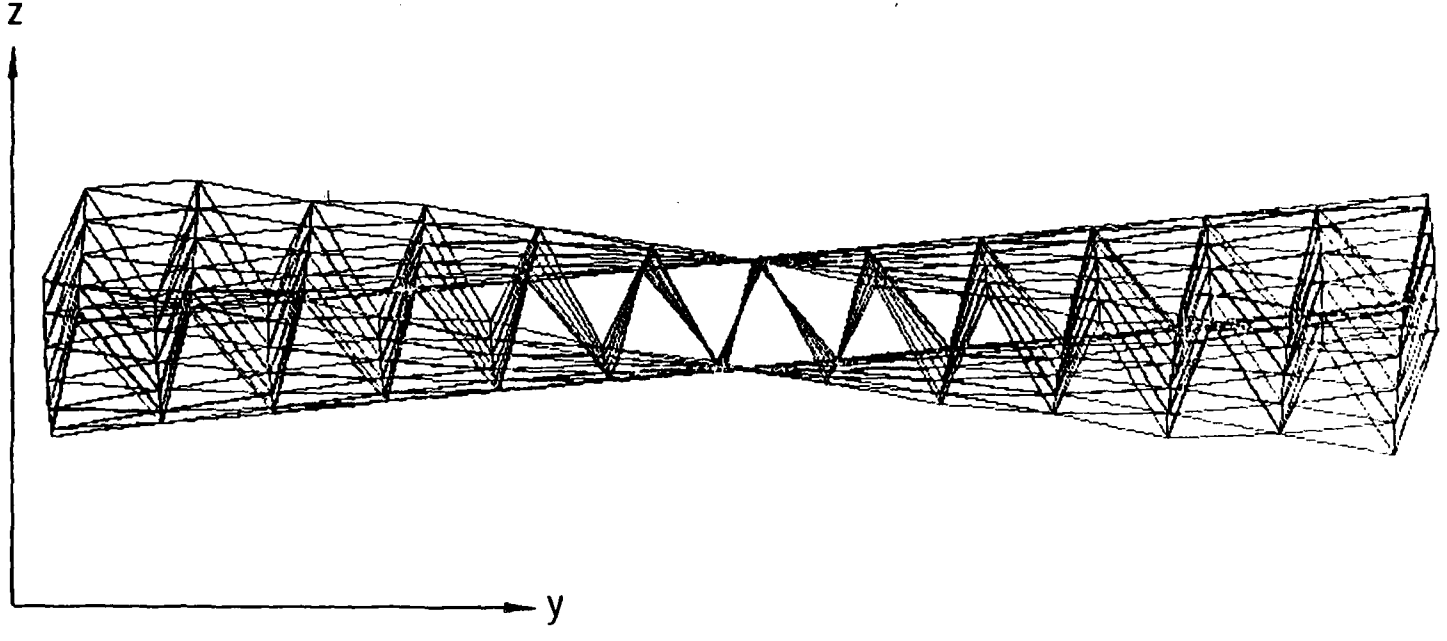

Fig. 42. Fourth Mode - Y-Z Plane Projection
(Free-Free Boundary Conditions)

V. CONCLUSIONS

A methodology is presented for modeling large truss-type structures based on the concept of equivalent continuum. The procedure for obtaining equivalent effective elastic and dynamic properties in terms of the material and geometric properties of the truss is simple and straightforward. A general three-dimensional equivalent continuum model is reduced, in the present study, to a two-dimensional plate through simple kinematic assumptions. The platform and the boundary conditions of the equivalent continuum plate model simulate those of the original truss structures. The effects of transverse shearing strain, rotary inertia, bending-extensional and inertia coupling are included in the continuum model.

Numerical results, presented in this study, are for a tetrahedral truss with simply supported and free-free boundary conditions. Whereas a closed form solution was obtained for the equivalent continuum plate with simply supported boundary conditions, the same was not possible in the case of a plate with free-free boundary conditions. The solution in the latter case was obtained using the NASTRAN computer program. The results adequately demonstrate the accuracy obtainable from the continuum model. In most instances, the error is less than 3 percent. Furthermore, the four solutions, I through IV, demonstrate the significance of including the transverse shear and rotary inertia terms. It is observed that the plate solution I, which includes both transverse shear and rotary inertia effects, is very good, even when the number of basic repeating truss elements is small.

For the truss with a small number of repeating elements, the effect of transverse shear is significant. As the number of the repeating elements increases, the transverse shear effect becomes less pronounced as shown in Figs. 8 through 15. The rotary inertia effect, on the other hand, is important only for higher frequency responses and for a smaller number of repeating elements. Yet, it is much less pronounced than that of the transverse shear (see Tables 5 through 12). Furthermore, the effect of transverse shear becomes much more

significant for the case in which $A_d = 0.05A$ as compared to the case in which $A_d = A$. The mode shapes of the truss with simply supported and free-free boundary conditions (see Figs. 16 through 24) exhibit striking similarity with those of a plate with similar boundary conditions. The main conclusions of the study are summarized as follows:

1. The technique of replacing a large truss structure with an equivalent continuum is extremely promising.

2. Good agreement between the discrete and its equivalent continuum model solutions can be obtained.

3. The classical plate solution may only be suitable for simple geometries with large numbers of repeating modules. For relatively small numbers of repeating truss elements, the transverse shear and rotary inertia effects must be included in the solution of the equivalent continuum model.

REFERENCES

1. "Outlook for Space," NASA Task Group, NASA SP-386, January 1976.

2. Hedgepeth, John M., "Survey of Future Requirements for Large Space Structures," NASA CR-2621, 1975.

3. Woods, A. A., Jr., "Offset Wrap Rib Concept and Development (LMSC)," Large Space Systems Technology, NASA Conference Publication 2118, 1979.

4. Archer, J. S., "Advanced Sunflower Antenna Concept Development (TRW)," Large Space Systems Technology, NASA Conference Publication 2118, 1979.

5. Montgomery, D. C. and L. D. Skides, "Development of Maypole (Hoop/Column) Deployable Reflector Concept for Large Space Systems Applications (Harris Corp.)," Large Space Systems Technology, NASA Conference Publication 2118, 1979.

6. "Modular Reflector Concepts Study (GDC)," Large Space Systems Technology, NASA Conference Publication 2118, 1979.

7. "DOD/STS On-Orbit Assembly Concept Design Study (GDC)," SAMSO-TR-78-128, 1978.

8. "DOD/STS On-Orbit Assembly Concept Design Study (MMC)," Martin Marietta Corporation, Report MCR-78-113, 1978.

9. Agan, W. E., "Erectable/Deployable Concepts for Large Space System Technology (Vought Corp.)," Large Space System Technology, NASA Conference Publication 2118, 1979.

10. Britton, W. R. and J. D. Johnston, "Space Spider - A Concept for Fabrication of Large Space Structures," AIAA Conference on Large Space Platforms: Future Needs and Capabilities, September 1978.

11. Stokes, J. W. and E. C. Pruett, "Structural Assembly in Space," Large Space Systems Technology, NASA Conference Publication 2118, 1979.

12. Nein, M. E. and F. C. Runge, "Science and Applications Space Platforms," AIAA 81-0458, AIAA Second Conference on Large Space Platforms, February 1981.

13. Johnson, R. R., H. Cohan, and G. G. Jacquemin, "A Concept for High Speed Assembly for Erectable Space Platforms," AIAA 81-0446, AIAA Second Conferece on Large Space Platforms, February 1981.

14. Stoll, H. W., "Systematic Design of Deployable Structures," AIAA 81-0444, AIAA Second Conference on Large Space Platforms, February 1981.

15. Dean, D. L. and R. R. Avent, "State of the Art of Discrete Field Analysis of Space Structures," Proceedings of Second International Conference on Space Structures, Edited by W. J. Supple, University of Surrey, Guildford, England, September 1975.

16. Renton, J. D., "The Related Behavior of Plane Grids, Space Grids, and Plates," Space Structures, Blackwell, Oxford, England, 1967.

17. Renton, J. D., "General Properties of Space Grids," International Journal of Mechanical Sciences, Vol. 12, 1970.

18. Dean, D. L. and C. P. Ugarte, "Field Solutions for Two-Dimensional Framework," International Journal of Mechanical Sciences, Vol. 10, 1968.

19. Mikulas, M. M. Jr., H. G. Bush, and M. F. Card, "Structural Stiffness Strength and Dynamic Characteristics of Large Tetrahedral Space Truss Structures," NASA TMX74001, 1977.

20. Bush, H. G., M. M. Mikulas, Jr., and W. L. Heard, "Some Design Considerations for Large Space Structures," Proceedings of the AIAA/ASME 18th Structures, Structural Dynamics, and Materials Conference, Vol. A, 1977.

21. Renton, J. D., "On the Gridwork Analogy for Plates," Journal of Mechanics, Physics, and Solids, Vol. 13, 1965.

22. Flower, W. R. and L. C. Schmidt, "Analysis of Space Truss as Equivalent Plate," Journal of the Structural Division, Vol. 97, ASCE, 1971.

23. Heki, K., "On the Effective Rigidities of Lattice Plates," Recent Researches of Structural Mechanics, Tokyo, 1968.

24. Sun, C. T. and T. Y. Yant, "A Continuum Approach Toward Dynamics of Gridworks," Journal of Applied Mechanics, Vol. 91, ASME, 1965.

25. Nayfeh, A. H. and M. S. Hefzy, "Continuum Modeling of Three-Dimensional Truss-Like Space Structures," AIAA Journal, Vol. 16, No. 8, 1978.

26. Nayfeh, A. H. and M. S. Hefzy, "Continuum Modeling of the Mechanical and Thermal Behavior of Discrete Large Structures," AIAA 80-0679, AIAA/ASME/ASCE/AHS 21st Structures, Structural Dynamics, Materials Conference, May 12-14, 1980.

AD-A119 349 AEROSPACE CORP EL SEGUNDO CA VEHICLE ENGINEERING DIV F/G 12/1
DEVELOPMENT OF AN ANALYTICAL MODEL FOR LARGE SPACE STRUCTURES.(U)
MAR 82 M ASWANI F04701-81-C-0082
UNCLASSIFIED TR-0082(9975)-1 SD-TR-82-59 NL

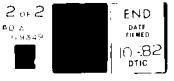

27. Fung, Y. C., Foundations of Solid Mechanics, Prentice-Hall, Inc., Englewood Cliffs, NJ, 1965.

28. Szilard, R., Theory and Analysis of Plates, Prentice-Hall, Inc., Englewood Cliffs, NJ, 1974.

29. Heki, K., "On the Effective Rigidities of Lattice Plates," Recent Researches of Structural Mechanics, Tokyo, 1968.

30. Reissner, E., "The Effect of Transverse Shear Deformation on the Sending of Elastic Plates," Journal of Applied Mechanics, Vol. 12, June 1945.

31. Mindlin, R. D., "Influence of Rotary Inertia and Shear on Flexural Motions of Isotropic, Elastic Plates," Journal of Applied Mechanics, Vol. 18, No. 1, March 1951.

32. Mindlin, R. D., A. Schacknow and H. Deresiewicz, "Flexural Vibrations of Rectangular Plates," Journal of Applied Mechanics, Vol. 23, No. 3, September 1956.

33. MacNeal, R. H., "A Simple Quadrilateral Shell Element," Computer and Structures, Vol. 8, 1978.